sustainability

MDPI

Article

Targeting Energy Efficiency through Air Conditioning Operational Modes for Residential Buildings in Tropical Climates, Assisted by Solar Energy and Thermal Energy Storage. Case Study Brazil

Alex Ximenes Naves [1,2], Laureano Jiménez Esteller [3], Assed Naked Haddad [4,*] and Dieter Boer [2]

[1] Programa de Pós-Graduação em Engenharia Civil, Universidade Federal Fluminense, Rua Passo da Pátria 156, Niterói 24210-240, Brazil; axnaves@id.uff.br
[2] Departament d'Enginyeria Mecànica, Universitat Rovira i Virgili, Av. Països Catalans 26, 43007 Tarragona, Spain; dieter.boer@urv.cat
[3] Departament d'Enginyeria Química, Universitat Rovira i Virgili, Av. Països Catalans 26, 43007 Tarragona, Spain; laureano.jimenez@urv.cat
[4] Departamento de Construção Civil, Escola Politécnica da Universidade Federal do Rio de Janeiro, Av. Athos da Silveira Ramos 149, Rio de Janeiro 21941-909, Brazil
* Correspondence: assed@poli.ufrj.br; Tel.: +55-21-2562-7962

Abstract: Economy and parsimony in the consumption of energy resources are becoming a part of common sense in practically all countries, although the effective implementation of energy efficiency policies still has a long way to go. The energy demand for residential buildings is one of the most significant energy sinks. We focus our analysis on one of the most energy-consuming systems of residential buildings located in regions of tropical climate, which are cooling systems. We evaluate to which degree the integration of thermal energy storage (TES) and photovoltaic (PV) systems helps to approach an annual net zero energy building (NZEB) configuration, aiming to find a feasible solution in the direction of energy efficiency in buildings. To conduct the simulations, an Energy Efficiency Analysis Framework (EEAF) is proposed. A literature review unveiled a potential knowledge gap about the optimization of the ASHRAE operational modes (full storage load, load leveled, and demand limiting) for air conditioning/TES sets using PV connected to the grid. A hypothetical building was configured with detailed loads and occupation profiles to simulate different configurations of air conditioning associated with TES and a PV array. Using TRNSYS software, a set of scenarios was simulated, and their outputs are analyzed in a life cycle perspective using life cycle costing (LCC). The modeling and simulation of different scenarios allowed for identifying the most economic configurations from a life cycle perspective, within a safe range of operability considering the energy efficiency and consequently the sustainability aspects of the buildings. The EEAF also supports other profiles, such as those in which the occupancy of residential buildings during the day is increased due to significant changes in people's habits, when working and studying in home office mode, for example. These changes in habits should bring a growing interest in the adoption of solar energy for real-time use in residential buildings. The results can be used as premises for the initial design or planning retrofits of buildings, aiming at the annual net zero energy balance.

Keywords: energy efficiency; optimization; solar energy; thermal energy storage; residential air cooling; variable rate energy tariffs; life cycle costing

Citation: Naves, A.X.; Esteller, L.J.; Haddad, A.N.; Boer, D. Targeting Energy Efficiency through Air Conditioning Operational Modes for Residential Buildings in Tropical Climates, Assisted by Solar Energy and Thermal Energy Storage. Case Study Brazil. *Sustainability* **2021**, *13*, 12831. https://doi.org/10.3390/su132212831

Academic Editor: Paulo Santos

Received: 26 October 2021
Accepted: 16 November 2021
Published: 19 November 2021

1. Introduction

For the building energy efficiency analysis, the definition of the systems, establishing their physical frontiers and the time frame, can bring the most different and, in some cases, controversial results. Expanding those system frontiers that envelop the whole building,

including eventual internal energy sources, allows for the analysis of the technical and economic feasibility that aims to reduce the life cycle cost (LCC) and to increase the building energy autonomy in relation to the grid.

Net zero energy buildings (NZEB) can be understood as buildings that, for a given time, generate as much energy as they consume. Either from the point of view of supply or consumption, energy availability is related to some basic issues such as source(s), conversion, distribution, utilization, waste, optimization, efficiency, and autonomy. These issues reveal the complexity of the subject of energy and justify the special attention given to it by the academic community.

We evaluate in our study the degree to which the integration of thermal energy storage (TES) and photovoltaics (PV) conduct to NZEB configuration, aiming to find a feasible solution in the direction of energy efficiency in buildings. To conduct the simulations, an Energy Efficiency Analysis Framework (EEAF) is proposed. Although typical occupancy profiles have been adopted in these studies, the EEAF also supports other occupancy profiles, such as those in which the occupancy of residential buildings during the day is increased due to significant changes in people's habits, when working and studying at home office mode, for example. These changes in habits should bring a growing interest in the adoption of solar energy for real-time use, maybe affecting the configuration of residential buildings in the near future.

We focus on residential buildings located in regions of tropical climate. The tropics cover up to 40% of the earth's surface and are home to around 40% of the world population (estimated at around 50% by 2030), which experiences average temperatures between 20 °C to 30 °C (extremes of up to 40 °C) and precipitation above 1500 mm/year, which contributes to relative humidity above 70%, usually causing thermal discomfort for people.

Our goal is to show that refrigeration, being one of the most energy-consuming systems, can have its efficiency increased if it is associated with photovoltaic panels (PV). This allows for demand response management, taking advantage of the expressive duration of daytime exposure (10 to 13.5 h a day) and thermal energy storage systems (TES) to support the cooling demand resulting from the typical occupancy profile of residential buildings, concentrated in periods of absence of sunlight.

In this energy efficiency model, the NZEB approach drives to adjust the energy efficiency of their most energy-consuming systems and optimizes their operation, taking into account the characteristics of external energy sources (e.g., variable electricity grid tariffs) associated with the use of internal energy sources (PV).

The effects of including PV were also analyzed for conventional and variable electricity tariffs. The PV associated with the cooling systems allowed for demand response management, considering the substantial duration of exposure to sunlight in tropical regions and the demand for refrigeration during energy tariff peak periods in addition to allowing the TES to be charged even in the absence of sunlight, that is, during off-peak periods.

Reviewing documents published in sources such as the Scopus database, the state of the art of research carried out around the world on the topic of renewable energy applied to buildings can be verified. When using the search term combinations "photovoltaic" and "thermal energy storage" and "air conditioning" or "HVAC", for the fields "title", "abstract", and "keywords", the Scopus engine returned 149 documents published since 1980 as results. Only 14 documents were found up until 2010. A fact that stands out is that from 2017 to 2020, on average, 20 documents were published per year. This gives evidence of a growing interest of the scientific community in these topics.

To achieve net zero energy balance and more viable energy efficiency results, although solutions vary according to country characteristics, common results seem to indicate that the concept of energy efficiency is no longer related to the radical load disconnection procedure, but for a smarter use.

In their review, Yongbao, C. et al. [1] highlight how essential the demand response strategies are while adopting measures to improve energy demand flexibility for Chinese buildings. In the same line, Asano, H. et al. [2] described the saving potential of the demand

response strategy applied to Japanese buildings, though with some side effects for the comfort of occupants. Fiorentine, M. et al. [3] introduced the importance of thermal energy storage in order to improve the management of a solar assisted HVAC system, analysing an Australian residential base case.

Hirsch, A. et al. [4], from the National Renewable Energy Laboratory (NREL) in the USA, described how computer modeling plays a key role while dealing with multiple decision variables, from the preliminary design to the completed building. In their study, Sehar, F. et al. [5] emphasized the advantages of an integrated automation model in order to simulate the set of PV, TES, and HVAC applied for American demand responsive buildings. The aspect of PV intermittency was approached by Sivaneasan, B. et al. [6], proposing an algorithm for managing this issue using demand response management in Singaporean green buildings.

Solano, J. C. et al. [7] from Spain show the importance of managing the HVAC expressive energy demand in European buildings and propose the use of PV connected to the grid and a battery energy storage system with intelligent control in order to work around this issue. In the same line, Pombeiro, H. et al. [8] from Portugal proposed the use of dynamic programming and genetic algorithms to control HVAC systems, focusing the thermal comfort and energy cost reduction with PV and batteries, using Energy Plus for simulations. The use of genetic algorithms, via TRNSYS, for the sizing of a NZEB was proposed by Yu, Z. et al. [9] in their study for a Chinese case.

The literature review unveiled a potential knowledge gap on the optimization of operating modes proposed by ASHRAE (American Society of Heating, Cooling, and Air Conditioning Engineers) that are associated with grid-connected PV. The issue of exporting surplus photovoltaic energy, considering the grid as a virtual battery, that is, an external storage of electrical energy, also seems not to have been sufficiently explored. This study aims to fulfil these gaps.

ASHRAE operational modes, ref. [10] in addition to the autonomous operation of air conditioning, combines three more configurations that associate air conditioning with TES, called full storage load, load leveled, and demand limiting.

Aiming to conduct an optimization study of the space cooling systems, the TRNSYS 18 Simulation Software [11] was used to model a residential building and its main load components. Details about TRNSYS and its features are given in Appendix B. The simulations were conducted by shifting the operation of the cooling system to the off-peak periods and charging the TES. The TES is then used to support the cooling demand during the peak periods. The simulations consisted of variations in PV sizing and the air conditioning/TES operability modes proposed by ASHRAE and generated results that validate our proposition toward a NZEB, using input data, parameters from manufacturers, and standardized levels of comfort for the building occupants. Analyses of hourly-based annual climate data from Rio de Janeiro (23° S Latitude) in Brazil allowed us to verify the solar thermal effects in the buildings at tropical latitudes.

In this study, the demand response (DR) was adopted, simulating the effects of shifting the cooling energy consumption from the peak to the off-peak tariff hours. The main goal of these simulations was to find the operation energy rate and lowest cost. The power was also one of the main simulation results, not only for its weight on the sizing of the cooling system and electrical circuits but also because of its considerable part in the electricity tariffs.

The US National Action Plan on Demand Response [12] explains DR as a reduction in the consumption of electric energy by customers from their expected consumption in response to an increase in the price of electric energy or to incentive payments designed to induce lower consumption of electric energy. In the studies of Li et al. [13] arises the potential of DR schemes to manage energy for residential buildings in a smart grid context. However, the DR has as one of its main prerequisites the implementation of advanced metering (AM), which measures and records usage data at hourly intervals or more frequently, providing usage data to both consumers and energy companies at least once daily [12].

A central air-cooled chiller system was configured and associated with a TES, using water as an energy storage element. As pointed out by Sehar et al. [14], the cool energy can be stored in thermal energy storages (TES) in the form of ice, chilled water, eutectic solutions, or phase change materials during the nighttime and used in the daytime. Parameshwaran et al. [15] and Heier et al. [16] explain in their studies the most important strategies for charging and discharging a TES to meet cooling demand during peak hours: full-storage and partial-storage strategies.

The choice of the strategy is based on the characteristics of the cooling load. This approach was also adopted for the air chilled cooling system for the simulations, aiming at energy savings and operational optimizations, foreseeing also the electrical power sizing and the equipment's service life, without compromising the building cooling demand. The choice for a chilled water-based TES, despite its lower costs and good efficiency rates, was also influenced by the results described by Hasnain [17] in a review publication.

The Energy Efficiency Analysis Framework (EEAF) and its methodology to implement the simulations, the case study details, and the main results and conclusions are presented in this paper.

The novelty of this article lies in the above-mentioned framework, which includes the main steps to proceed with an energy efficiency analysis and their results, evolving the systems of air conditioning/TES and grid/PV, which reveals the feasibility of implementing a real NZEB. Improvements in the lighting and equipment of the building, although not included in the scope of this study, represent promising opportunities for future energy efficiency actions that are aiming to achieve the complete NZEB configuration.

2. Materials and Methods

Based on the Energy Efficiency Analysis Framework (EEAF), the application of this study followed the methodology according to the eight steps described in Appendix A. In this section, the four initial processes related to scoping, simulation models, objective functions to be minimized (e.g., annual costs, LCC, payback), optimizations, and sensitivity analysis are discussed. The Results and Discussion section addresses the last four processes related to the analysis of results, viable solutions, and proposed actions to implement energy efficiency measures with reliability. In the Conclusions, we discuss the reproducibility procedures and the conditions for the generalization of these studies and their results, understood as the applicability of this study of energy efficiency to other buildings.

2.1. Scope and System Boundaries

The scope for this study is the analysis of a tropical located residential building containing the main loads, namely lighting, equipment, and cooling, focusing on the optimization of that which is the most energy-consuming. The analyses of hourly-based, annual climate data were carried out for a building located in Brazil, at Rio de Janeiro (23° S Latitude).

2.2. Simulation Model, Scenarios, and Proceed Simulations

Due to the characteristics of the object of study, mainly because of the existence of a great number of independent variables, the use of equations relating to the system's variables is excessively and computationally time-consuming. However, the use of simulation software based on numerical calculation of models of well-known systems (e.g., buildings and their facilities) allows for the analysis of energy demand of these models, in addition to considering their behavior on the passage of time. Due to these reasons, TRNSYS 18 Simulation Studio and its optimization library component, GenOpt (Generic Optimization Program), were chosen.

The TRNSYS Simulation Model was configured in three main blocks:

- Hypothetical building model, initially designed in the SketchUp and configured via TRNSYS Building tool, for the calculation of the building cooling demand;

- Cooling system model, responsible to supply the building cooling demand and calculate the whole building electrical energy demand. This model simulates ASHRAE operational modes for the chiller/TES set and allows to choose each of the four selected scenarios;
- PV/grid model, responsible to supply the building electrical energy demand for the different scenarios and calculate the LCC and payback. Interacts with the GenOpt for the optimization process.

As mentioned above, for the energy efficiency studies, three blocks were configured and integrated into the TRNSYS model. The integration is a prerequisite to run the optimizations of the complete model by GenOpt.

First, a hypothetical building model was designed to obtain the electrical energy demand based on three main loads, that is, the cooling, the lighting, and equipment energy demand. The building electrical energy demand from lighting and equipment was obtained from standard load and occupation configuration, directly on the TRNSYS Type 56b. The 3D building model was created through the SketchUp Software and exported to the TRNSYS using an integration plugin.

After that, the building electrical energy demand from cooling was obtained through the cooling demand necessary to maintain the comfort of the apartments that were used as input to the chiller/TES model. This model allows for obtaining detailed data of each of the electrical energy demands corresponding to the different ASHRAE operational modes and changing these operational modes during the optimization process.

Finally, the PV/grid model was designed to allow for the simulations and optimizations of the different configurations of PV and grid as the supply of electrical energy, considering the three main loads of electrical demand obtained from the other two TRNSYS models, which the connection schema of can be seen in Figure 1. Note that type 9c described in the same figure is the integration point between this model and the other two models, reading the electrical energy demand from the building.

At TRNSYS, the building was represented in the simulation model as a Type 56b component, composed of zones defined during the drawing phase, connected with other types, such as weather information and unit calculation, and conversion tools, printers, plotters, cooling/heating systems, thermal energy storage, and grid electricity tariff information. Building location (hemisphere, position) inputs and outputs were also defined in the Type56b via TRN build editor, and each building zone was configured as an apartment, to allow the configuration of construction types (walls, floors, ceilings, rooves, windows, doors), scheduling (occupation, control of regime type components), and the regime types (infiltration, ventilation, heating, cooling, comfort, gains, losses, lighting, and daylight controls). These configurations can be implemented specifically for each zone or as a common parameter. The energy demands of the building, considering the cooling demand, lighting, and equipment, were imported by the PV model via Type 9c, as mentioned above and shown in Figure 1.

Modeling of the scenarios in TRNSYS uses modules, named types, which represent the main systems. The types used to build the TRNSYS models, as well as their functionalities, are described in Appendix B.

The TRNSYS model also considers the surplus energy produced by the PV but not consumed by the building loads, due to the exceeding production during the periods of most intensive solar radiation. An electricity tariff can be attributed to the surplus energy exported to the grid, which will reflect positively on the cost savings calculation and consequently in the LCC and payback period of the investments. The storage of the PV surplus energy and its use in other periods could also have been simulated. However, in this model, the option of exporting this energy to the grid in exchange for credits was included, which in other words corresponds to the use of external energy storage. PV array physical space demand, which can represent a restriction for PV installation on rooftops or in parking, is obtained by the simulations and the optimization process.

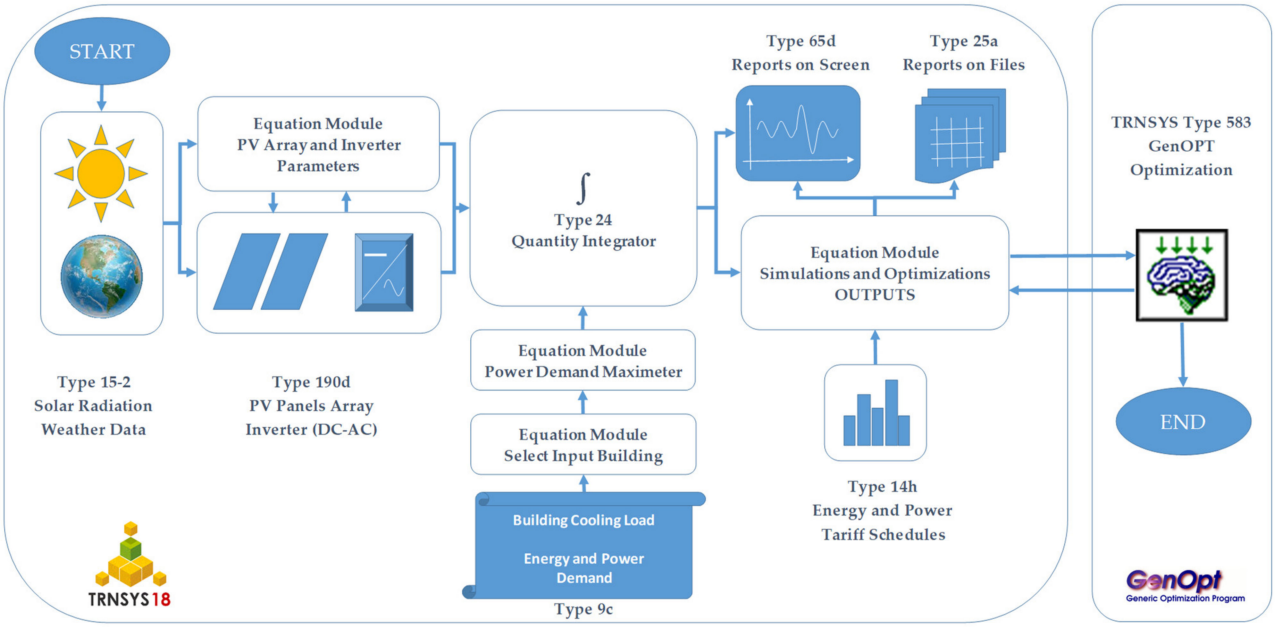

Figure 1. TRNSYS model for Energy Efficiency simulations and optimization.

Different scenarios were simulated and based on the principles of life cycle costing (LCC) and payback period, and GenOpt performed single-objective optimization (SOO) process, taking into account the life cycle economic aspects. The GenOpt plugin can read its input from text files generated by TRNSYS simulations and writes its output to text files. The independent variables can be continuous (possibly with lower and upper bounds), discrete, or both. Constraints on dependent variables can be implemented using penalty or barrier functions. GenOpt uses parallel computing to evaluate the simulations.

At the TRNSYS model was configured a forcing function to select the ASHRAE operational mode for the chiller and TES and also to switch the integration of PV and the grid for simulation and optimization. In order to run the simulations, besides the data requirements described above for each type of module in TRNSYS, some scenarios were considered, and some restrictions were taken into account. The three main loads of the building were the chiller, lighting, and equipment. The integration of the TES and chiller, running on each of the three ASHRAE operational modes (full storage load, load leveled, and demand limiting), and the PV connected to the grid were used to set up the four scenarios described below:

- Base Case: grid + chiller full capacity (no TES);
- Scenario 1: PV + grid + chiller partial time + TES full storage load;
- Scenario 2: PV + grid + chiller partial capacity + TES partial load (load leveled);
- Scenario 3: PV + grid + chiller partial capacity + TES partial load (demand limiting).

2.3. Objective Functions and Optimization

During the optimization process, the life cycle costing (LCC) and payback period were taken into account. Based on the principles of the life cycle economic aspects of the energy balance necessary to support the building energy demand, the GenOpt performed a multi-objective optimization (MOO) process for the distinct scenarios, aiming to determine mainly the global minimum of the objective function LCC. However, the global minimum payback period, PV energy (production, consumption, and surplus), and grid energy consumption were also obtained through the same TRNSYS/GenOpt model.

The LCC basic calculation formulas are presented in Equations (1) and (2). The present value of LCC, named LCC, was adopted for the comparison of the different scenarios and as the decision support tool, calculated as follows.

$$LCC(t,i,C) = \sum_{t=0}^{N} \frac{C_t}{(1+i)^t} \quad (1)$$

where:

C_t = Sum of all relevant costs occurring in year t (EUR);
N = Length of study period (years);
i = Nominal discount rate (%).

The real discount rate (r), considering the inflation rate (I), was calculated from Equation (2).

$$i = (1+r)\cdot(1+I) - 1 \quad (2)$$

where:

r = Real discount rate (%);
i = Nominal discount rate (%);
I = General energy price inflation (%).

For the LCC calculations, considering Brazil, annual values for the nominal discount rate of 7.00% and an energy price inflation rate of 3.50% were adopted, resulting in a real discount rate of 3.38%, obtained through Equation (2). The time frame for the life cycle was 20 years.

The simulation data collected on an hourly basis allow for the direct calculation of power (kJ/h or kW) and energy (kJ or kWh). These data were used as input to the central cooling system based on air-cooled chiller and the TES. The electricity from the grid was used to supply the energy demand integrated with the PV panels, mainly to support the cooling energy demand during the mid-peak and off-peak periods and to charge the TES to support the building cooling demand during the peak periods.

2.4. Sensitivity Analysis

As stated by T. El Hajji et al. [18], the sensitivity analysis can be conducted using different approaches based on a quantitative method, as published by Y. Zheng [19], or a qualitative method, as shown by N. Stroe et al. [20].

In this study, the use of GenOpt integrated with the TRNSYS model made it feasible to adopt a sensitivity analysis that consisted in the definition of a base case situation, taking into account qualitative aspects (e.g., consider producing PV array surplus energy to export to the grid) and quantitative aspects (e.g., introduce price variations on the grid energy tariff). Once the base case has been established, the next step is to run the optimization process introducing an intervention, which could be the insertion of a new independent variable or a variance in an existing variable, leaving all other assumptions and input variables unchanged. In this way, after running the optimization, it was possible to obtain the variance of the output variable (e.g., LCC). The sensitivity values should be normalized in a percentage to have the same range of variation, allowing one to categorize and compare the input variables according to their influence in the output variable.

As indicated by Sozer et al. [21], it is also important to identify the requirements to produce variations with their sensitivity to each other, to minimize unexpected side effects in advance, for example, the PV array can have its costs significantly increased if a structure to control the tilt angle of the panels is considered, although this control results in a reduction in the LCC.

It is important to note that a life cycle perspective through the application of life cycle cost (LCC) allows for the comparison of different scenarios, extending the period of analysis beyond the initial investments and unveiling the trade-offs necessary to justify the decisions. The payback period can also support the decision-making process.

Steps 5 to 8 of the EEAF, named respectively Analyse Results and Solutions, Set the Solution Reliability and Validity, Discuss the Reproducibility Procedures, and Discuss the Solution Generalisation are self-explanatory and are inserted in Section 4, Results and Discussion, and Section 5, Conclusions.

3. Case Study

3.1. Building Description

A building model was configured to allow the simulation of the cooling demand and the sizing of the air-cooled chiller system and a thermal energy storage (TES).

A brief layout, drawn in Trimble SketchUp and later exported to the TRNSYS platform, can be seen in Figure 2. The building thermal properties are given in Appendix C and Tables A2–A4 as well as a sample of the building cooling demand (Figure A2).

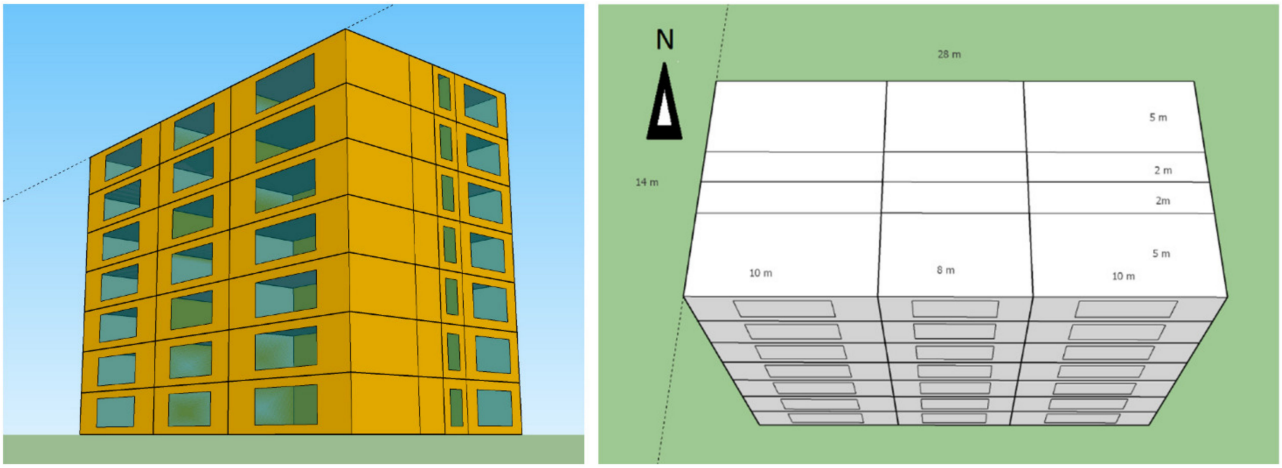

Figure 2. Building scheme and orientation.

3.2. Grid Electricity Tariffs

The variable tariff (hours of the day, seasons of the year) has been adopted by several countries. The Spanish seasonal tariffs, for example, have been implemented gradually, aligned with the liberalization of the energy market in Europe since 2009 [22,23], and the Brazilian white tariff for residential customers was implemented in 2018, according to the Brazilian National Electrical Energy Agency [24]. In Table 1 are shown the Brazilian flat and variable energy tariff, named the conventional (C) and variable tariff (V), respectively, where the peak, mid-peak, and off-peak times can be observed. For these tariffs, it was not considered a seasonal variation in prices.

Table 1. Variable (V) and conventional (C) tariffs.

Tariff Types	Period (h)		Price	
Variable Tariff/Conventional	**Workday**	**Weekend**	**Energy (EUR/kWh)**	**Power (EUR/kW/day)**
V–P1–Peak	18–21		0.109321	0.0334758
V–P2–Mid Peak	17–18/21–22		0.086337	0.0167380
V–P3–Off Peak	0–17/22–24	0–24	0.059067	0.1413472
C–Conventional	0–24	0–24	0.067621	0.1915610

The energy and power values for workdays and weekends, used for the calculations, are shown in Table 1.

3.3. Building Cooling Demand Profile

The building model was configured with occupation, lighting, and equipment loads, as shown in Figure 3, and adjusted with air conditioning information to support comfort levels according to [22].

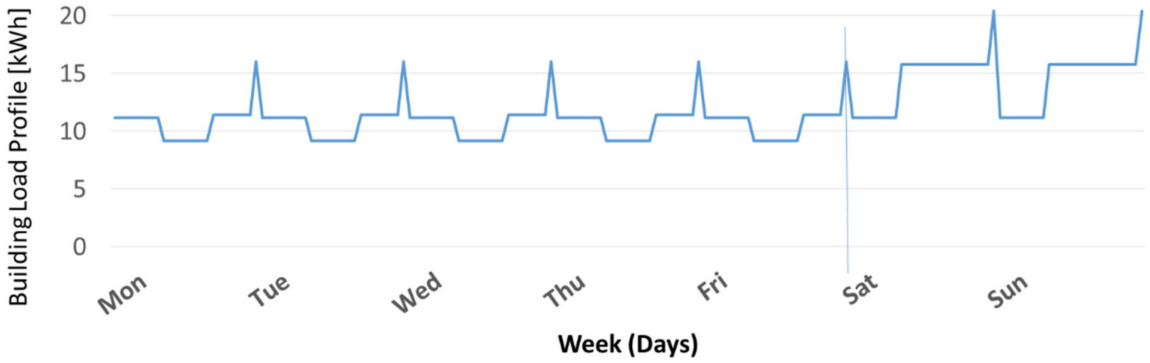

Figure 3. Building weekly load profile (kWh).

3.4. Cooling System Overview

A model was built in the TRNSYS Simulation Studio to simulate the air-cooled chiller and the TES simulations, which are described below for each of four of the ASHRAE operational modes. A single model was allowed to perform the optimizations in TRNSYS and GenOpt, considering the operational mode itself as a variable to be tested. The control signals are described according to the loop they belong to.

The main items of the cooling system included in the model are shown in Figure 4 and described below:

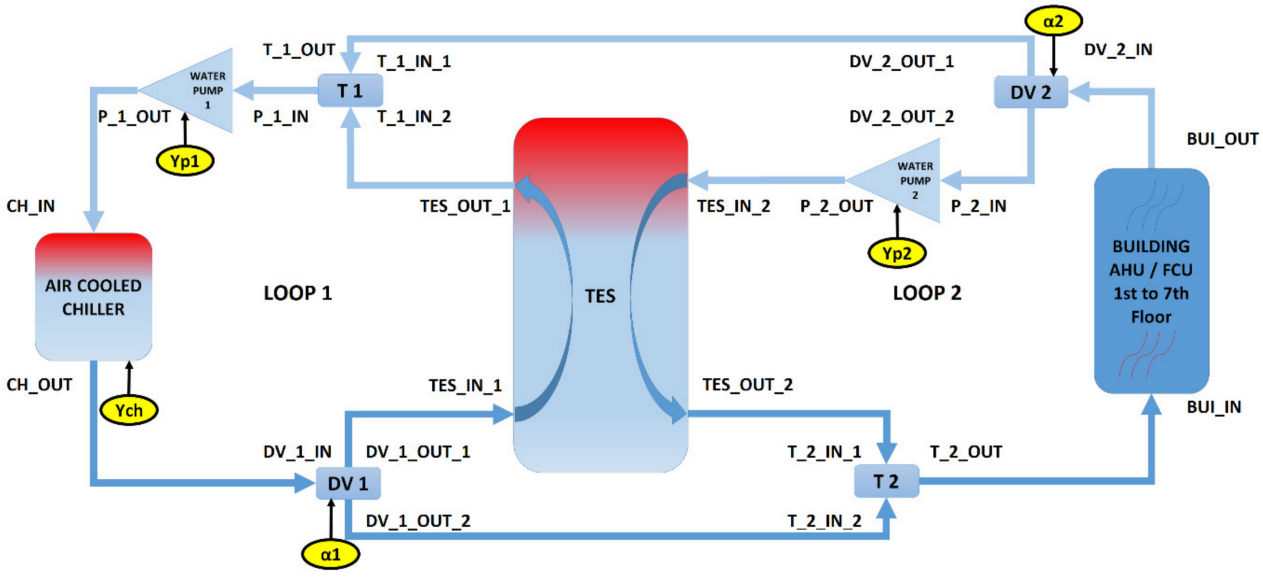

Figure 4. Air-cooled chiller, TES, and building air handling units (AHU).

Loop 1

- Air-cooled chiller (condenser, evaporator, and cooling fans);
- Variable speed pump (chilled water);
- Thermal energy storage—TES_IN_1 and TES_OUT_1.

Loop 2

- Thermal energy storage—TES_IN_2 and TES_OUT_2;
- Variable speed pump (chilled water);
- Building air handling unit (AHU) and fan coil unit (FCU).

The condenser is commonly located on the roof and exchanges the heat from the building using ambient air circulated and forced by fans through its coils, which are integrated to an evaporator that uses a normal water closed loop as refrigerant distributed to the AHU/FCU. The pumps, evaporator, and TES can be located on the roof or inside the building. The system performance depends mainly on the energy losses from the chilled water closed loop used for transferring the cooling energy and the sensible dry bulb outdoor temperature. If the temperature increases, the building load increases and the chiller performance decreases; if the temperature decreases, the building load decreases. and the chiller performance increases. For this reason, the operation of the chiller, in the scenarios with TES, has better performance during nights.

- Loop 1: the chiller and pump work based on signals (schedule and the TES top temperature);
- Loop 2: the pump works based on the signal (the required water amount for building load demand).

The water pump operation signal changes the water flow rate to deliver the amount required to supply the cooling demand, using Equations (3) and (4) for the signal value, which is between 0 to stop the pump and up to 1 for 100% of the pump capacity. The TES volume defines the stored energy from the hourly cooling load calculation and can be obtained from basic thermodynamic equations considering a temperature range, ΔT of 5 K.

All the cooling energy calculations were based on the water flow on an hourly basis. The adopted simulation time step of one hour allows the water flow rate (m^3/h) to be easily obtained.

Table 2 shows the main control signals, illustrated in Figure 4.

Table 2. Main control signals.

		Base Case	Scenario 1	Scenario 2	Scenario 3
Loop 1	Y_{ch}	$CH_{Cap\ 0}$.(1.AND.(Q_{BCD} > 0))	$CH_{Cap\ 1}$.(1.AND.($TES_{DL} > 0$))	$CH_{Cap\ 2\ or\ 3}$.(CH_{Sch}.AND. ((Q_{BCD}.OR.TES_{DL}) > 0))	
	Y_{p1}	1.AND.($Q_{BCD} > 0$)	1.AND.($TES_{DL} > 0$)	CH_{Sch}.AND.((Q_{BCD}.OR.TES_{DL}) > 0)	
	α_1	0	1	$CH_{IntRate\ 2\ or\ 3}$.($Q_{BCD} - TES_{DL}$)	
Loop 2	Y_{p2}	0	α_1.AND.($Q_{BCD} > 0$)	α_1. ($Q_{BCD} - TES_{DL}$)	
	α_2	α_1	α_1	α_1	

Y_{ch} = *Chiller*; Y_{p1} = *Water Pump* 1; α_1 = *Divisor* 1; Y_{p2} = *Water Pump* 2 ; α_2 = *Divisor* 2. TES_{DL} = 1.AND.($TES_{TopTemp}T > 5$ [°C]; $CH_{InitCap}$ =110.8 [kW].

A brief description of the simulation scenarios based on the cooling demand aspect is presented below. In Figure 5, the different ways that each air conditioning operating mode works can be compared. For the Base Case (operational mode 0, Figure 5a) the chiller operates in a period of the day to support the building cooling demand. For Scenario One (operational mode 1, Figure 5b), the chiller loads the TES during the off-peak periods, and the building cooling demand is supported mainly by the TES. The chiller also operates during a period of the day.

For Scenarios Two and Three (operational modes 2 and 3, Figure 5c,d) the chiller operates 24 h a day and divides with the TES the task of supporting the building cooling demand.

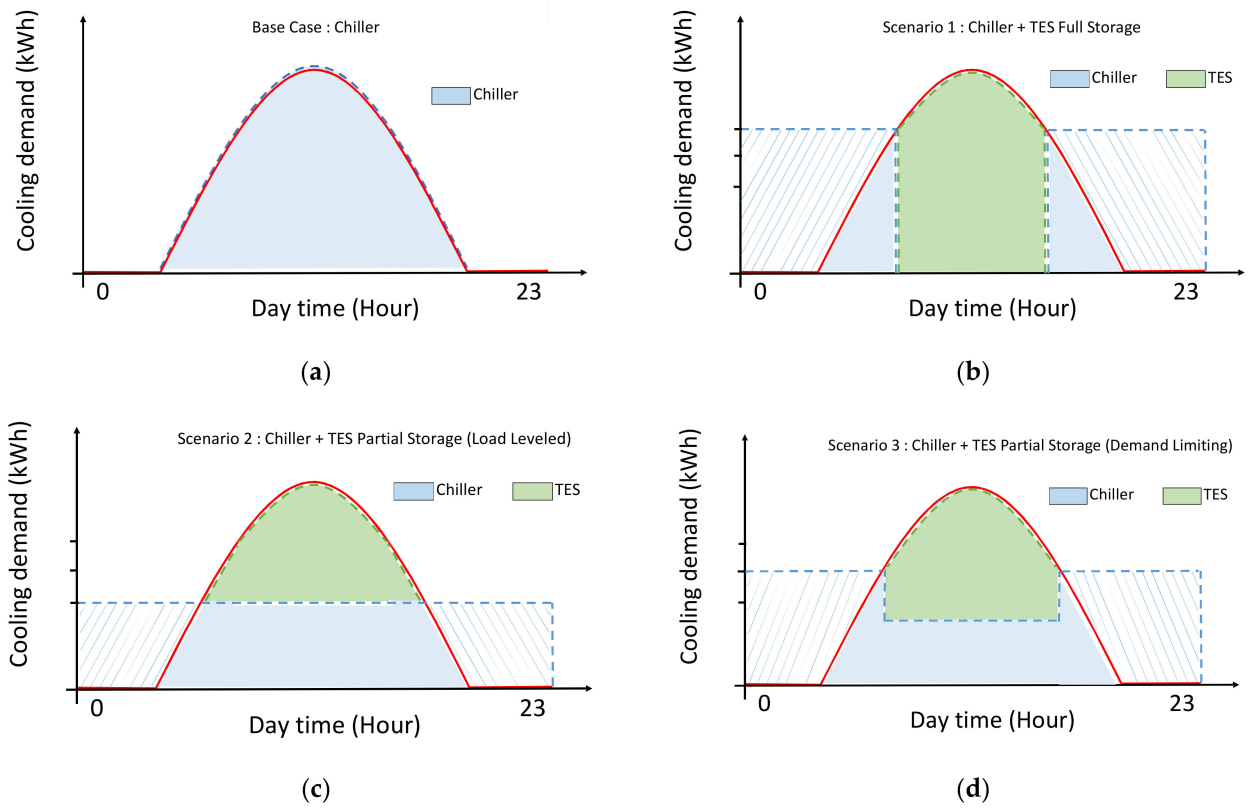

Figure 5. Cooling demand supply for (**a**) Base Case, (**b**) Scenario 1, (**c**) Scenario 2, and (**d**) Scenario 3.

3.4.1. Base Case—Chiller Only (No Storage)

In the Base Case scenario, Loop 1 and Loop 2 are connected, and the TES is out of operation. For energy-consuming comparison purposes, this configuration is the Base Case. This configuration, by hypothesis, would be the best configuration to take advantage of solar energy, due to the simultaneity between the chiller load requirement and the insolation level.

The cooling system without TES (see Figure 6a) consists of one pump to circulate the cooled water between the chiller and cooling coil, and the system works based on the load demand signals.

The control signal for water pump one is obtained from Equation (3).

$$Y_{p1} = \frac{m_1}{m_{max}} = \frac{m_2}{m_{max}} = \frac{m}{m_{max}} = \frac{Q_{BCD}}{C_p \cdot \Delta T} \cdot \frac{1}{m_{max}} \quad (3)$$

where:

Y_{p1} = Signal control value of Water Pump 1 at LOOP 1 $[0 \leq Y_{p1} \leq 1]$;
Q_{BCD} = Building cooling demand (kWh);
$m_2 = m_1 = m$ = Water mass necessary to supply the building cooling demand (kg);
F_{rMax} = Pump flow rate capacity kg/h or m^3/h;
C_p = Specific heat for water;
ΔT = Cool coil temperature difference $(T_{out} - T_{in})$ (°C).

Considering Q for the hottest hour, B_{CD} of the hottest day, represented as Q_{Build_max} detailed in Equation (4), can be determined as the most adequate chiller capacity necessary to supply the building cooling demand.

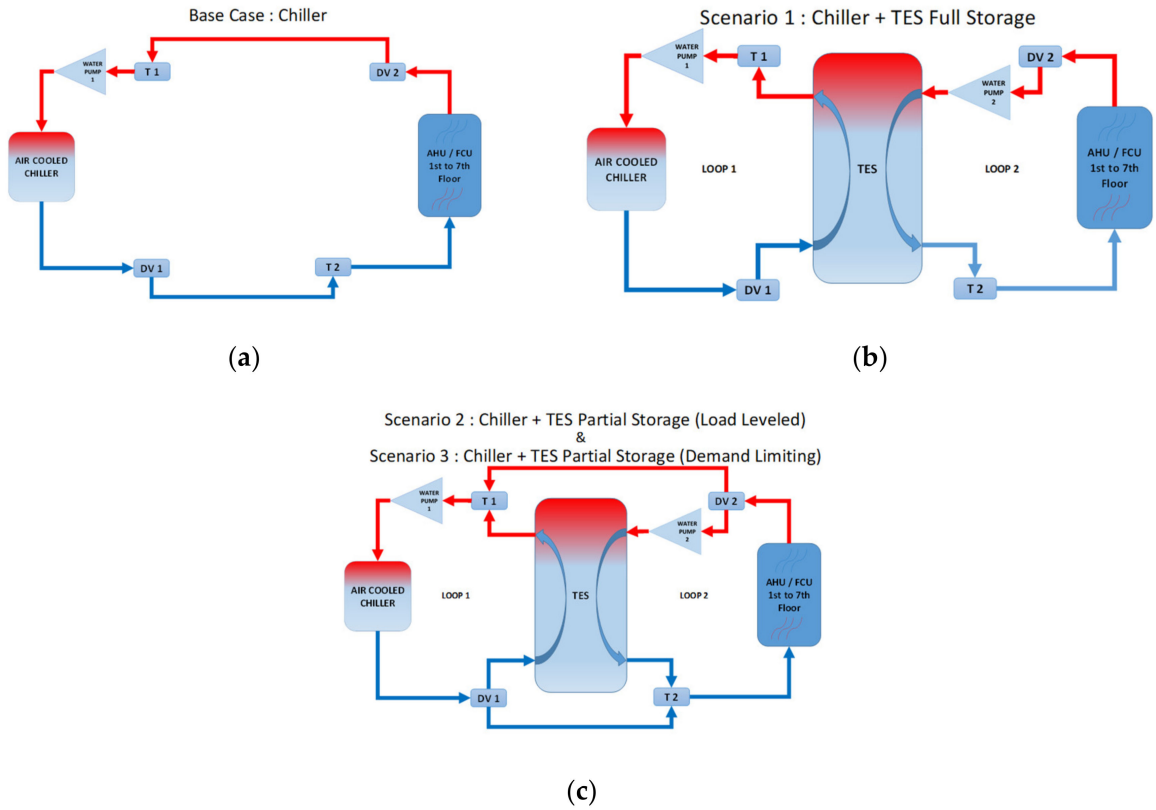

Figure 6. (**a**) Base case—chiller only (no storage); (**b**) Scenario 1; (**c**) Scenarios 2 and 3.

This value can be used to validate the theoretical formula for the chiller sizing, based on building and climate parameters (e.g., USA DOE chiller sizing guidelines [25]).

Equation (4) also allows for determining the pump capacity m_{max}, that is, m_{HH} in kg. The m_{max} divided by the water density (ρ) results in the pump capacity in m^3/h, as described in Equation (5).

$$Q = m \cdot C_p \cdot \Delta T \ (Hottesthour) \ or \ Q_{Build\_max} = m_{HH} \cdot C_p \cdot \Delta T \tag{4}$$

$$m_{max} = m_{HH} = \frac{Q_{Build\_max}}{C_p \cdot \Delta T} \ or \ F_{rMax} = \frac{m_{max}}{\rho} \tag{5}$$

The chiller and water pump one dimensions are obtained via the partial TRNSYS simulation results.

From the TRNSYS building model (Type 56b) simulations, considering the climate data from Rio de Janeiro, Brazil and the typical loads for lighting, equipment, and occupation, the maximum hourly cooling demand load was $Q_{Build\_max} = 110.61$ kWh. These results obtained from the TRNSYS building model on an hourly basis also allows for obtaining the cooling capacity (power) of the chiller for the ASHRAE operational mode 1, with no TES, used as the Base Case for this study, that is 110.61 kW or 31.45 ton. Additional data about the chiller can be seen in Appendix D and on the manufacturer's website [26].

Considering $\Delta T = 5$ [K] and using Equation (6), the maximum chilled water mass (m_{max}), or the volume (F_{rMax}) to be pumped from the chiller to the building cool coil to supply the air handling units/fan coil units, can be obtained.

$$m_{max} = \frac{Q_{Build\_max}}{C_p \cdot \Delta T} = \frac{110.61}{1.165 \times 10^{-3} \times 5} = 18,989 \left[\frac{kg}{h}\right] \text{ or } F_{rMax} = \frac{18,989}{1000} = 18.9 \left[\frac{m^3}{h}\right] \tag{6}$$

where:

Q_{Build_max} = Building maximum cooling demand (kWh);

C_p = Specific heat for water (kWh/kg°C);
ΔT = Cool coil temperature difference ($T_{out} - T_{in}$) (°C);
Fr_{Max} = Pump flow rate capacity kg/h or m^3/h;
ρ = Water density (kg/m^3).

3.4.2. Scenario 1—Chiller Full Capacity + TES Full Storage Load

At the cooling system with a TES (see Figure 6b), the loop is divided into two loops, one between the TES and chiller for charging the TES with cooling energy by decreasing its temperature, and the other between the TES and cooling coil to supply the load demand. The heat will be exchanged by the air from the load to decrease the air temperature and increase the cooling water temperature to move back to the TES.

The initial value for the TES volume, Equation (7), and dimension, Equation (8), used to start the simulations of Scenario One (chiller full capacity and TES full storage load) was calculated based on the maximum daily load obtained from the TRNSYS building model (3843.36 MJ or 1067.60 kWh). This value was optimized during the simulations for the different operational modes evolving the chiller and the TES, according to the simulation Scenarios One, Two, and Three.

$$V_{TES} = \frac{Q_{Build\_max\_d}}{C_p \cdot T \cdot \rho} = \frac{1067.60}{1.165 \times 10^{-3} \times 5 \times 1000} = 183.28 \left[m^3\right] \quad (7)$$

$$H_{TES} = 2 \cdot \sqrt[3]{\frac{2 \cdot V_{TES}}{\pi}} = 2 \cdot \sqrt[3]{\frac{2 \cdot 183.28}{\pi}} = 9.77 \text{ m} \quad \textit{and} \quad D_{TES} = \frac{H_{TES}}{2} = \frac{9.77}{2} = 4.89 \text{ [m]} \quad (8)$$

where:

V_{TES} = TES volume (m^3);
$Q_{Build\_max\_d}$ = Building maximum cooling demand (kWh/day);
C_p = Specific heat for water (kWh/kg °C);
ΔT = TES temperature difference ($T_{out} - T_{in}$) (°C);
ρ = Water density (kg/m^3);
H_{TES} = TES height [m], calculated to be twice of D_{TES} = TES diameter [m].

3.4.3. Scenario 2—Chiller Partial Capacity + TES Partial Storage (Load Leveled)

In this scenario (see Figure 6c), the chiller is set to work in a leveled capacity necessary to support the building cooling demand during the off-peak periods and load the TES, which will be discharged during the peak periods of cooling demand.

3.4.4. Scenario 3—Chiller Partial Capacity + TES Partial Storage (Demand Limiting)

In this scenario (see Figure 6c), the chiller is also set to work in a leveled capacity necessary to support the building cooling demand during the off-peak periods. However, the chiller capacity is limited during the peak periods of cooling demand, requiring a higher capacity during the off-peak periods to supply enough load to the TES, which will be discharged during the peak periods of cooling demand.

The main variables handled to improve the simulation scenarios and to achieve the goals were:

- Chiller capacity and chiller operation schedule;
- TES volume and height;

The chiller price considered was based on the market parameter value of 560 EUR/ton and maintenance of 8.72 EUR/ton/year. For the TES, a parametric price of 100 EUR/m^3 was considered [27] and an annual maintenance cost of 0.08 EUR/m^3, resulting in an annual maintenance cost for the whole refrigeration system of 8.80 EUR/ton [28].

3.5. PV System Overview

The average efficiency of the PV panels for this case study was 11.7%, with a module efficiency of 13.4% [29] and an inverter efficiency of 91.5% [30]. Every single panel occupies a surface of 1.64 m^2 and must be connected in parallel sets of seven panels each (the separate sets are connected in series). This distribution is advisable for security purposes and to equalize the DC voltage to the input range of market inverters (e.g., the solar inverters list published by NATA, the National Association of Testing Authorities [30]).

The complete list of the PV specifications and the main electrical specifications used to configure the PV component (type 190) on the TRNSYS model, according to the calculation method presented by DeSoto et al. [31], can be found on the manufacturer's website [29]. From these data, both the values of maximum installed power supplied by the panels and their costs can be calculated. For example, 12 sets (of seven panels) equate to 86 panels of 220 Wp, providing a maximum power of 18.2 kWp, for 38 sets we would have 58.5 kWp, and so on. Through parametric costs calculations (EUR/Wp), where the average prices of panels were extracted from the benchmark issued by the National Renewable Energy Laboratory (NREL) [32] using the most economical values, that is, 0.68 EUR/Wp the cost of the panels was calculated, as well as their annual maintenance cost, estimated by the same source at 0.02 EUR/Wp.

4. Results and Discussion

4.1. Analyze Results and Solutions

For the Base Case, the cooling load for the building is supplied by a chiller of 31.2 ton, a commercial value close to that capacity calculated in the Case Study section for the Base Case.

In Scenario One, the simulations unveiled that a TES with 75% of the calculated value in the Case Study was adequate to maintain the building temperatures at the desired range across the year. This was considered with a TES with a storage tank capacity of 137.46 m^3 to feed the cooling load for the building, the details of which can be found in the manufacturer's catalog [27]. The chiller of 31.2 ton operates during the night with a full capacity ratio and charges the TES that delivers cooling to the building.

Based on the results of Scenario One, Scenarios Two and Three were optimized and configured with a smaller TES of 110.07 m^3 and a chiller of 15.6 ton, which would be adequate to maintain the building temperatures at the desired range across the year. In Scenario Two (load leveled), the chiller operates up to 24 h a day with the capacity ratio set to 75% of maximum cooling load, and it charges the TES that delivers cooling to the building. When demand is lower than 75%, the surplus energy will be stored in the TES, and when demand exceeds limitations, the TES supplies the excess cooling demand.

In Scenario Three (demand limiting), the chiller also operates 24 h a day. However, the limitation of the chiller during the higher demand loads, necessary to supply the cooling demand, was set to 65% after the simulations. Although it represents the annual energy consumption better than Scenario Two, as shown in Table 3, when considering the PV integration, Scenario Two takes more advantage of the insolation and consequently brings more savings, as shown below.

Table 3. Annual results of the simulation scenarios.

	Tariffs			Energy Demand (MWh)			Power Demand (kW)				Annual Costs (EUR)			
	Var/ Conv	Hour/ Year	% Cool	Cool	Light/ Equip	Total En.	Cool	Light/ Equip	Total Pw.	Optm Ct.Pw	Energy Cost	Power Cost	Total Cost	Annual Saving
Base Case	P1	1095	10.4	9.9	9	18.9	34.3	8.2	42.5	35	6685.46	2338.55	9024.02	1.10%
	P2	730	7.9	7.6	6	13.5	36.8	8.2	45	30				
	P3	6935	19.4	18.6	44.7	63.3	33.6	13.6	41.8	37				
	C	8760	37.7	36.1	59.7	95.8	36.8	13.6	45	40	6473.92	2651.51	9125.43	0.00%
Scen. 1	P1	1095	0.2	0.2	9	9.2	0.7	8.2	8.9	9	6426.45	2141.91	8568.35	6.10%
	P2	730	0.2	0.2	6	6.2	0.8	8.2	8.9	9				
	P3	6935	40.7	41.2	44.7	85.9	32.1	13.6	45.6	42				
	C	8760	41	41.5	59.7	101.2	32.1	13.6	45.6	42	6843.04	2741.37	9616.49	−5.0%

Table 3. *Cont.*

	Tariffs			Energy Demand (MWh)			Power Demand (kW)				Annual Costs (EUR)			
	Var/ Conv	Hour/ Year	% Cool	Cool	Light/ Equip	Total En.	Cool	Light/ Equip	Total Pw.	Optm Ct.Pw	Energy Cost	Power Cost	Total Cost	Annual Saving
Scen. 2	P1	1095	8.5	8	9	17	12.7	8.2	20.9	19				
	P2	730	5.7	5.4	6	11.4	13.1	8.2	21.3	20	6442.72	1324.12	7766.84	14.90%
	P3	6935	22.9	21.7	44.7	66.4	13.1	13.6	23.7	22				
	C	8760	37.1	35.1	59.7	94.8	13.1	13.6	23.7	22	6409.43	1454.26	786,369	13.80%
Scen. 3	P1	1095	9.4	8.9	9	17.2	8.7	8.2	16.9	17				
	P2	730	5.9	5.6	6	11.6	9.1	8.2	17.3	16	6273.61	1401.99	7675.6	15.90%
	P3	6935	22.7	21.6	44.7	66.3	13.5	13.6	27.1	24				
	C	8760	37.2	35.4	59.7	95.1	13.5	13.6	27.1	24	6342.62	1615.49	7958.11	12.80%

4.1.1. Base Case—PV + Grid + Chiller (No Storage)

The Base Case was configured with a chiller of 31.2 ton dimensioned to support the cooling demand of the whole building, located in Rio de Janeiro, Brazil. The simulations with variable tariffs resulted in more expenses compared to the initial simulations with conventional tariffs, evidencing the need for a detailed analysis by the customers before contracting these tariffs. The energy consumption concentrated on the most expensive period driven by the building cooling demand, and the demanded power levels of operation justified these results, as shown in Figure 7, which shows the day with the highest cooling demand.

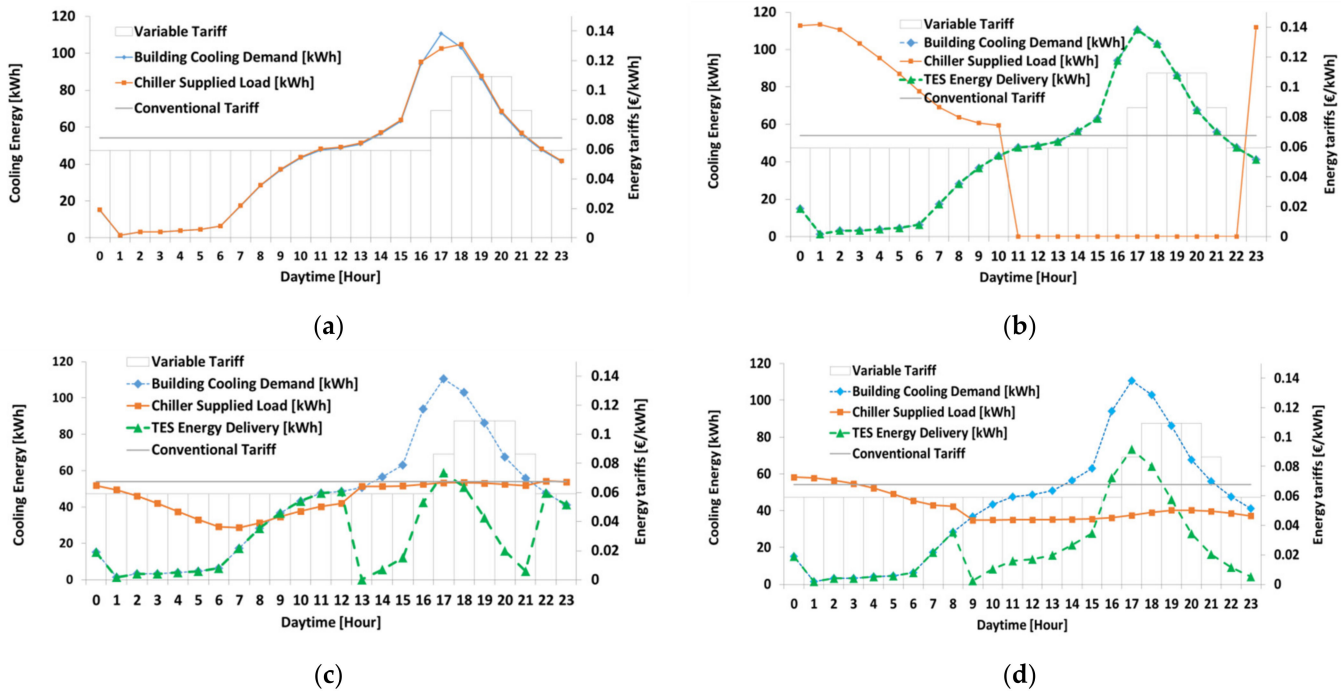

Figure 7. (**a**) Base Case—chiller (no storage); (**b**) Scenario 1—chiller partial time + TES full storage load; (**c**) Scenario 2—chiller partial capacity + TES partial load (load leveled); (**d**) Scenario 3—chiller partial capacity + TES partial load (demand limiting).

Compared to the other building electrical loads, detailed in Table 3, the chiller was responsible for 36% of the building energy consumption and for almost 80% of the electrical power demand, which would represent the main load for the electrical circuits dimensioning. However, even this initial central cooling configuration of 31.2 ton and an initial investment of EUR 17,500, if compared to conventional distributed cooling solutions, is most economic. In few numbers, the 42 units would demand about 70 individual pieces of equipment of 1 ton, a total of 70 ton, which would cost about EUR 31,500, based on a

market parameter value of 450 EUR/ton [33]. This is not mentioning the lower coefficient of performance, the higher energy demand, power capacity, environmental impact, and maintenance costs.

4.1.2. Scenario 1—PV + Grid + Chiller + TES Full Storage Load

The simulation results of the Base Case allowed for the dimension and configuration on TRNSYS 18 of a TES of 137.46 m^3 with a chiller of 31.2 ton working in its full load, which was necessary to completely shift the cooling demand from the peak tariffs. The results are shown in Figure 7b. In this configuration, the energy consumption, as detailed in Table 3, was responsible for 40.2% of the building energy consumption and 70% of the electrical power demand. This scenario represented annual energy savings of 7.6% when operating in a variable tariff context, but the elevated power capacity and the LCC analysis revealed that more improvements could be carried out.

4.1.3. Scenario 2—PV + Grid + Chiller Partial Capacity + TES Partial Load (Load Leveled)

The analysis of Scenario One allowed us to verify that the energy consumption could be decreased to achieve a smooth distribution of the energy necessary for supporting the cooling demand with less power capacity. Figure 7c illustrates the results for this configuration. The chiller works 24 h a day and during the night supplies energy to the TES, which discharges this energy during the peak period, contributing to the support of the building cooling demand.

The annual energy consumption obtained at Scenario One of 40,279 kWh, if distributed across the 8760 h of the year, would result in a smaller chiller. The TRNSYS model was initially configured with a chiller of about 50 kW found in the manufacturer's manual [26]; more precisely, the chiller was 15.6 ton or 56 kW. For this new scenario, from Equation (7), a smaller TES volume was also obtained from the TRNSYS model simulations, that is, 110.07 m^3.

Table 3 shows the results of these simulations related to the energy and power demand. In Scenario Two, the chiller power reached 14 kW, and in Scenario Three it reached 9 kW due to the demand limiting operation mode. Figure 7c,d allow for the comparison between the load leveled and demand limiting operation modes and the effects on the performance of the chiller and the TES to support the building cooling demand.

4.1.4. Scenario 3—PV + Grid + Chiller Partial Capacity + TES Partial Load (Demand Limiting)

After the simulations of Scenario Two, the chiller operation was changed to a limited capacity during the peak cooling demand period, as shown in Figure 7d. This configuration, called Scenario Three, is the most energy-saving, representing a 15.9% reduction in the energy annual costs.

4.1.5. Annual Energy and Power Analysis (No PV energy)

The implementation of a TES associated with a chiller brought savings up to 14.9% in the annual energy cost, as shown in Table 3 for Scenario Two (load leveled) in the configuration of variable-rate tariffs. Moreover, Scenario Three (demand limiting) presented relevant savings, demonstrating the flexibility that the use of TES brought when combined with a chiller, even using only the grid as an energy source before the insertion of PV on the simulations.

4.1.6. PV Energy Analysis

Different scenarios were simulated, and the analysis of the results allowed for savings in initial annual costs in energy consumption of up to 14.9% and a reduction in the configuration of power circuits of up to 45%. The insertion of grid-connected PV increased annual energy cost savings by up to 33.8%, with a solar fraction of about 28%, without considering the export of surplus energy. However, the most efficient scenarios were obtained consider-

ing the production and export of the PV energy surplus, increasing annual cost savings by up to 67.8%.

During optimizations, for the best scenario, considering a net metering configuration [34], which generally limits the amount of monthly excess energy exported to the network to the amount of energy consumed in the previous month, the optimal annual solar fraction reached 42%, and another 58% of the energy consumed from the grid allowed an export of excess photovoltaic energy of up to 51%, using the grid as an external electrical energy storage of more than half of the energy consumed by the model building in one year.

For example, if the total annual energy consumed by the building was 100 MWh (39 MWh of cooling and 61 MWh of lighting and equipment), 58 MWh would be consumed from the grid and the PV could produce 83 MWh, of which 42 MWh would be to supplement the building's annual demand and the other 51 MWh could be exported to the network throughout the year, generating credits and savings.

As shown in Figure 8a, even on a warm summer day (8 January), with the optimization based on the minimum LCC, the energy efficiency aspect can be verified and also results in a minimum energy surplus (blue), and the total energy produced by the PV (red) is consumed (orange).

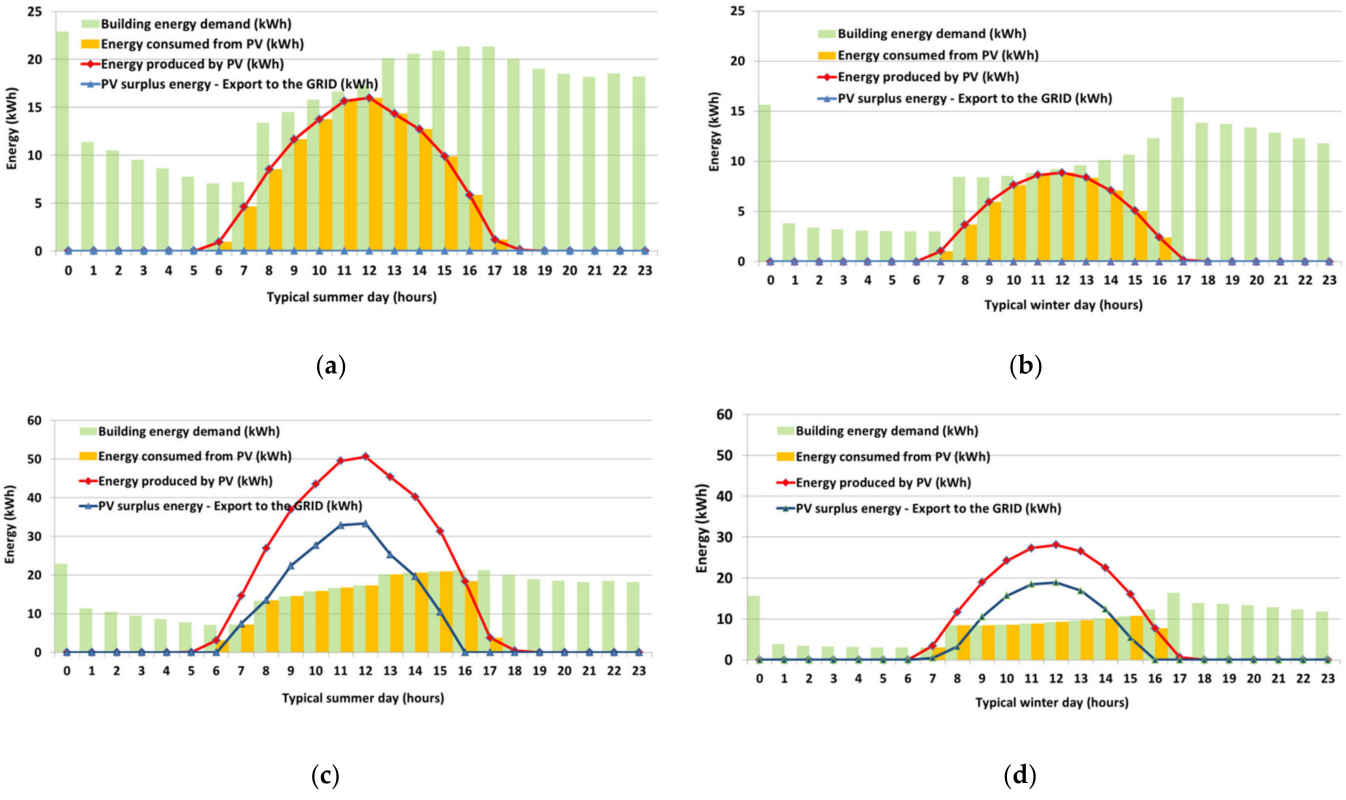

Figure 8. PV energy production versus building energy demand. (**a**) No PV surplus energy exported to the grid—summer; (**b**) no PV surplus energy exported to the grid—winter; (**c**) PV surplus energy exported to the grid—summer; (**d**) PV surplus energy exported to the grid—winter. Extracted from Scenario 2 (chiller, TES, load leveled, PV).

For a winter day (8 July), Figure 8b shows that the PV energy production is also adequate for the lower energy consumption, mainly because of lower cooling demand.

If the solar energy exportation is considered, the optimization, which is aiming for a minimum LCC, also results in an efficient model where all the PV surplus energy is exported to the grid, respecting the limits imposed by the net metering rules. Figure 8c shows this configuration for the same scenario, and the same day is drawn in Figure 8a.

For a winter day (8 July), the same day of Figure 8b, at Figure 8d it can be verified that the PV energy production is also adequate for the lower energy consumption, mainly because of lower cooling demand. However, the PV surplus energy is exported to the grid.

4.1.7. Life Cycle Costing Analysis

The annual energy savings analysis was improved with the use of LCC (present value of LCC) to justify an eventual investment in PV panels.

An optimization using the TRNSYS model and the GenOpt, changing the PV sizing and the ASHRAE operational modes for the chiller/TES set, aiming at the minimum LCC for a period of 20 years, as an objective function, showed the advantages of Scenario Two (chiller + TES partial load—load leveled) using 12 × 7 PV panels. These results are shown in Figure 9a,b (conventional and variable tariffs, respectively).

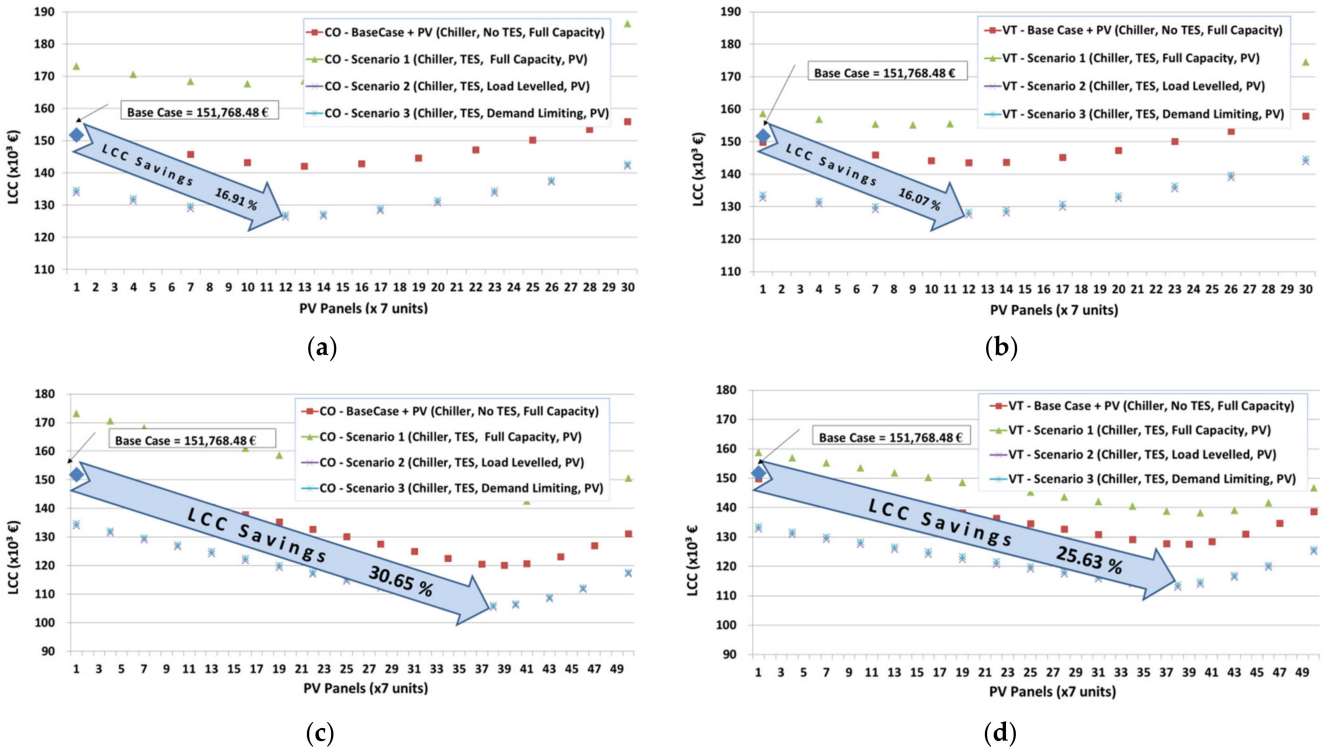

Figure 9. LCC analysis for scenarios. (**a**) No PV surplus energy exported to the grid (CO); (**b**) no PV surplus energy exported to the grid (VT); (**c**) PV surplus energy exported to the grid (CO); (**d**) PV surplus energy exported to the grid (VT).

If the solar energy surplus exportation to the grid is considered, the feasible number of solar panels to be installed increases from 84 (12 × 7) to 266 (38 × 7). Through the same optimization using the TRNSYS model and the GenOpt, changing the PV sizing and the ASHRAE operational modes for the chiller/TES set, and aiming at the minimum LCC for a period of 20 years, as an objective function, Scenario Two (chiller + TES partial load—load leveled) using 38 × 7 PV panels was the most economic. These results are shown in Figure 9c,d (conventional and variable tariffs, respectively). The main TRNSYS simulation and optimization results for the Base Case and Scenarios can be verified in Appendix G.

From a life cycle point of view, the results also emphasize the energy efficiency aspect and the sustainability of the solution simulated in Scenario Two by contracting the conventional tariff (CO), Figure 9c, achieving LCC savings of up to 30.65%.

4.1.8. Payback Period Analysis

The payback periods for Scenario Two, considering the LCC savings showed in the last section, were lower than 8 years, as shown below.

Even before considering the PV integration, Figure 10 shows Scenario Two with the conventional tariff, which is the most money-saving scenario considering the LCC perspective and the effect of TES implementation, load leveled. If only the effect of TES implementation is considered, with no chiller reduction dimension, the payback period (orange) is lower than 10 years.

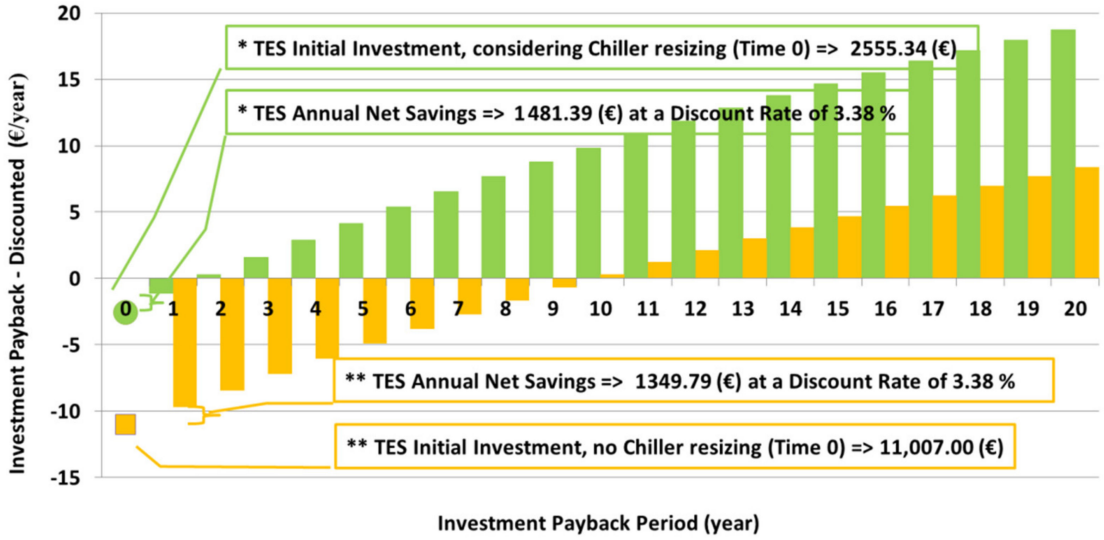

Figure 10. Scenario 2: Decreasing the TES payback period when considering the chiller capacity resizing. (*) Chiller resizing, (**) No Chiller resizing.

However, if the chiller reduction is considered, the payback period (green) falls to less than 2 years. We highlight here the positive effect of the TES implementation associated with the chiller.

The annual energy savings is 14.89%, annual net savings is 16.3%, and LCC savings is 12.34%.

For Scenario Two with the conventional tariff (see Figure 11), which is the most money-saving scenario considering LCC perspective, if the PV panels implementation is considered, even with no energy surplus exportation, the initial investment in 84 panels (12 × 7 panels) for the payback period is lower than 7 years (orange). For this configuration, the TES implementation and the chiller reduction sizing effects are also considered.

The annual energy savings is 33.82%, annual net savings is 31.11%, and LCC savings is 16.91%. The annual average solar fraction reaches 28.46%.

Finally, for Scenario Two, with the conventional tariff, which is the most money-saving scenario considering LCC perspective, if the PV surplus energy exportation is considered, for the initial investment in 266 panels (38 × 7 panels) the payback period is lower than 8 years, also shown in Figure 11. For this configuration, the TES implementation and the chiller reduction sizing effects are also considered.

The annual Energy savings rise to 79.26% and, considering the annual maintenance expenses, represent an annual net savings of 67.78%. The LCC savings is 30.65%.

At this configuration, considered the most energy-efficient and sustainable, the annual average solar fraction reaches 41.97%.

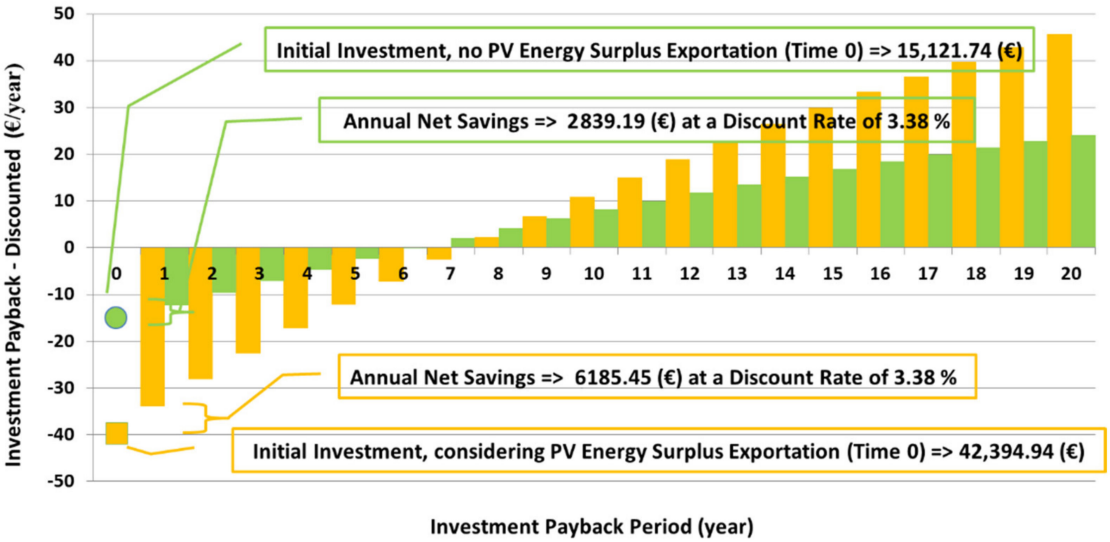

Figure 11. Scenario 2: Payback period with no PV energy surplus exportation (12 × 7 panels) and considering PV energy surplus exportation (net metering) (38 × 7 panels).

5. Conclusions

Important issues related to the energy efficiency of buildings, that is, the cooling demands and the energy storage, were detailed, discussed, and addressed considering the most recent initiatives related to the demand response. The proposed scenario proved that the cooling system, because of its partial load operation, can have its efficiency and lifetime increased when associated with thermal energy storage systems.

The adopted approach, using progressive simulation scenarios, has the potential to bring the most positive results with fewer efforts, once the built model is modular and expansible. The same approach can be adopted for other aspects of buildings, such as lighting, equipment, construction materials, alternative energy sources, and so on, towards a zero-energy balance in buildings.

The use of TRNSYS for configuring a building with detailed construction characteristics, input data from real equipment, and accurate weather information allowed us to reach the initial objectives proposed for these studies and to envisage the applicability of the results in the decision-making process related to one of the most energy-consuming systems of buildings. The optimization process, via GenOpt integrated to TRNSYS 18, allowed for the improvement of the initial results and unveiled the potential of this method, even when the number of alternatives was high, as with the PV sizing.

The results of modeling, simulation, and optimization can support an eventual design phase of the feasible solutions and foreseen advantages, disadvantages, restrictions, and opportunities with technological and economic aspects in a life cycle approach. The main methods (tools) that support this study, the reasons for its adoptions, the way they were applied, and how they can be reproduced were presented here.

Author Contributions: Conceptualization, A.X.N. and D.B.; data curation, A.X.N. and D.B.; formal analysis, A.X.N. and D.B.; funding acquisition, L.J.E.; investigation, A.X.N.; methodology, A.X.N., A.N.H. and D.B.; project administration, A.N.H. and D.B.; resources, D.B.; software, A.X.N.; supervision, A.N.H. and D.B.; validation, L.J.E. and D.B.; visualization, L.J.E.; writing—original draft, A.X.N.; writing—review and editing, A.X.N., L.J.E., A.N.H. and D.B. All authors have read and agreed to the published version of the manuscript.

Funding: This research was funded by the Spanish Government (RTI2018-093849-B-C33 MINECO/FEDER, UE), the Brazilian Government via CAPES/Brazilian Coordination for the Improvement of Higher Education Personnel (88881.134710/2016-01), and by CNPq/Brazilian National Council for Scientific and Technological Development. This work is partially funded by the Ministerio de Ciencia, Innovación y Universidades—Agencia Estatal de Investigaci'on (AEI) (RED2018-102431-T).

Institutional Review Board Statement: Not applicable.

Informed Consent Statement: Not applicable.

Data Availability Statement: Not applicable.

Acknowledgments: This article has been made possible through the support of the Ministerio de Economía y Competitividad (MINECO). The authors at the Universitat Rovira i Virgili would like to thank the Catalan Government for the quality accreditation given to their research group (2017 SGR 1409) and the financial support from the Spanish Ministry of Economy and Competitiveness (RTI2018-093849-B-C33 MINECO/FEDER, UE).

Conflicts of Interest: The authors declare no conflict of interest. The funders had no role in the design of the study, in the collection, analyses, or interpretation of data, in the writing of the manuscript, or in the decision to publish the results.

Nomenclature

AHU	Air Handling Unit
AM	Advanced Metering
ASHRAE	American Society of Heating, Cooling, and Air Conditioning Engineers
CO	Conventional Electricity Tariff
DOE	Department of Energy
DR	Demand Response
EEAF	Energy Efficiency Analysis Framework
FCU	Fan Coil Unit
HVAC	Heating, Ventilating, and Air Conditioning
GENOPT	Generic Optimization Program
GRID	Electrical grid
LCC	Life Cycle Costing
MOO	Multi-objective Optimization
NM	Net Metering
NREL	National Renewable Energy Laboratory
NZEB	Net Zero Energy Building
PB	Payback Period
PV	Photovoltaic
TRNSYS	Transient System Simulation Program
SHGC	Solar Heat Gain Coefficient
SOO	Single Objective Optimization
TES	Thermal Energy Storage
VT	Variable Electricity Tariff
WWR	Window-to-Wall Ratio

Appendix A. Energy Efficiency Analysis Framework (EEAF)

As stated by Schneider [35] and previously endorsed by Rudestam and Newton [36], these methods are the practical hands-on steps for performing a study and the methodology is the discussion of these methods. The methods usually include defining the scope of the research project, coming up with a research question or hypothesis, selecting and collecting data, processing that data with certain tools to enable analysis, and then going through the data systematically to answer the central question.

Besides the existence of some frameworks for the energy efficiency analysis in the literature, as published by D. Schachinger et al. [37], L. Friedrich and A. Afshari [38], A. J. Satchwell et al. [39], and I. Iskin and T. U. Daim [40], the planning of this study

unveiled needs that led the authors to propose a generic framework, which is expected to be useful to the energy efficiency analysis of other buildings.

The requirements mentioned above were organized into an Energy Efficiency Analysis Framework (EEAF) aiming to establish a comprehensive structure of the main steps adopted to reach the results of this study and their distribution in the whole document. The EEAF (see Figure A1) allowed the clear definition of the necessary processes, input/output data, analysis procedures, tools, and related activities to operationalize this energy efficiency study.

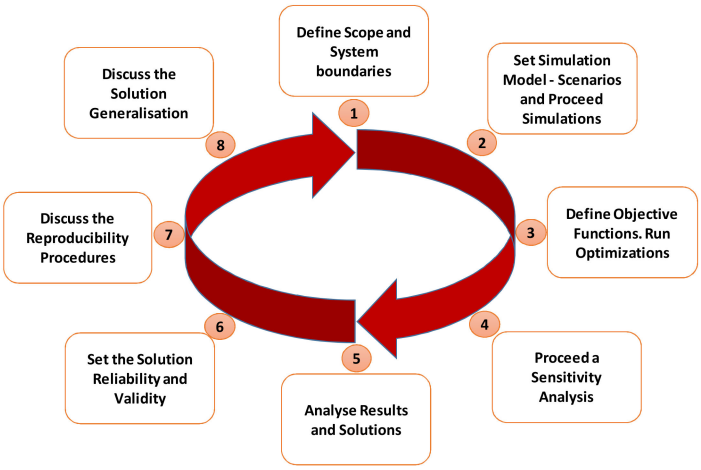

Figure A1. Energy Efficiency Analysis Framework (EEAF) processes 1 to 8.

Appendix B. Main TRNSYS Components

The types used to build the TRNSYS models are briefly described below, with some specific characteristics, to justify their utilization, and also help the reader eventually reproduce their functionalities in similar modeling studies. More details about TRNSYS and up to date versions can be found at the TRNSYS developer's web site [11].

Table A1. Main TRNSYS components.

Model: Name	Description	Function
Type 15-2: Weather Data Processor	Combines data reading, radiation processing, and sky temperature calculations.	Simulates the solar energy potential as input for the PV array using Energy Plus Weather Data [41] from different locations (Brazil) on an hourly basis for one year.
Type 56b: Building	Aggregates the information from the building model drawn in the Trimble SketchUp 2016 software and exported via 3DTrnsys plugin to TRNSYS Simulation Studio.	Simulates the residential building energy and power demand on an hourly basis for one year. Supply energy and power inputs to Type 9c.
Type 9c: Data Reader for Generic Data Files	Serves the purpose of reading data at regular time intervals from a data file, converting it to a desired system of units, and making it available to other TRNSYS components.	Reads the electrical hourly energy and power data files.
Type 190d: PV Array MPPT and Inverter (DC to AC)	Determines the electrical performance of a photovoltaic array, based on the calculation method presented by DeSoto et al. [31].	Simulates different array configurations categorized into scenarios to support the building energy demand.
Type 14h: Time-Dependent Forcing Function	Employs a time-dependent forcing function, which has a repeated pattern. Discrete data points indicating the value of the function at various times throughout one cycle (e.g., one day) set the pattern of the forcing function.	Sets the Variable Tariff Schedule for the energy and power contracted to calculate the costs and proceed with the life cycle cost and payback optimizations for the different scenarios.

Table A1. *Cont.*

Model: Name	Description	Function
Type 24: Quantity Integrator	Integrates a series of quantities over a period. Each quantity integrator can have up to 500 inputs. It can reset either periodically throughout the simulation or after a specified number of hours or after each month of the year.	Summarizes the amount of energy consumption, power demand, and life cycle costing.
Type Equation: Algebraic, Logic, and Boolean Equations	Allows implementing calculations and formulas using equations.	Calculates the output integrated values from Type 24 (Integrator) and implement logical conditions for the different scenarios related, for example, to the use of solar energy or grid energy to support the energy consumption and power demand. It also calculates the life cycle costing and payback period of possible investments for each scenario.
Type 65d: Reports on screen	Allows visualization of the graphical results of the simulations at different time frames (e.g., hourly based graphics for 8760 h of simulation, or 1 year).	Displays simulations in real-time.
Type 25a: Printer—TRNSYS	Supplies units printed to an output file.	Exports the simulation and calculation results
Type 583: GenOpt Optimazation	Optimization program for the minimization of a cost functionthat is evaluated by the TRNSYS Simulation Studio.	The cost function is the function being optimized. The cost function measures a quantity that should be minimized, such as a building's annual operation cost, a system's energy consumption, or a norm between simulated and measured values in a data fitting process. The cost function is also called the objective function.

Appendix C. Building Thermal Properties

Table A2. Material (layers).

Material	Conductivity (kJ/hmK)	Capacity (kJ/kgK)	Density (°C)	Resistance (hm^2K/kJ)
PLASTER_BOARD	0.576	0.84	950	-
FBRGLS_ASHRAE	0.144	0.84	12	-
WD_SIDN_ASHRAE	0.504	0.90	530	-
TIMBER_FLOOR_ASHRAE	0.504	1.20	650	-
RFDCK_ASHRAE	0.504	0.90	530	-
CONCRETE_SLAB	4.068	1.00	1400	-
INS_FLR_ASHRAE (Massless Layer)	-	-	-	6.965

Table A3. Properties of windows.

Window Type	WWR (%)	SGHC (%)	U-Value (W/m^2K)
Exterior Window 1	30	78.9	2.89
Exterior Window 2	30	78.9	2.89
Adjacent Window 1	30	78.9	2.89
Adjacent Window 2	30	78.9	2.89

Table A4. Thermal properties of walls, floors, ceilings, and rooves.

Wall Type	Material	Total Thickness (m)	U-Value (W/m^2K)
Boundary Wall		0.090	0.508
	PLASTER_BOARD	0.012	
	FBRGLS_ASHRAE	0.066	
	PLASTERBOARD	0.012	

Table A4. *Cont.*

Wall Type	Material	Total Thickness (m)	U-Value (W/m^{2}K)
Adjacent Wall		0.090	0.508
	PLASTER_BOARD	0.012	
	FBRGLS_ASHRAE	0.066	
	PLASTERBOARD	0.012	
Exterior Wall		0.087	0.510
	PLASTER_BOARD	0.012	
	FBRGLS_ASHRAE	0.066	
	WD_SIDN_ASHRAE	0.009	
Exterior Roof		0.141	0.316
	PLASTER_BOARD	0.010	
	FBRGLS_ASHRAE	0.112	
	RFDCK_ASHRAE	0.019	
Exterior Floor		0.030	0.039
	TIMBER_FLOOR_ASHRAE	0.030	
	INS_FLR_ASHRAE		
Boundary Ceiling		0.080	4.153
	CONCRETE_SLAB	0.080	
Adjacent Ceiling		0.080	4.153
	CONCRETE_SLAB		
Boundary Floor		0.030	0.039
	TIMBER_FLOOR_ASHRAE	0.030	
	INS_FLR_ASHRAE		
Ground Floor		0.080	0.039
	CONCRETE_SLAB	0.080	
	INS_FLR_ASHRAE		

The weather input data from Rio de Janeiro, Brazil, were used for the simulations. The building cooling demand necessary to meet comfort levels highlights the possibility of optimization to avoid periods of more expensive energy tariffs or to smooth the electricity needs for cooling, whether in summer or winter, as shown in Figure A2.

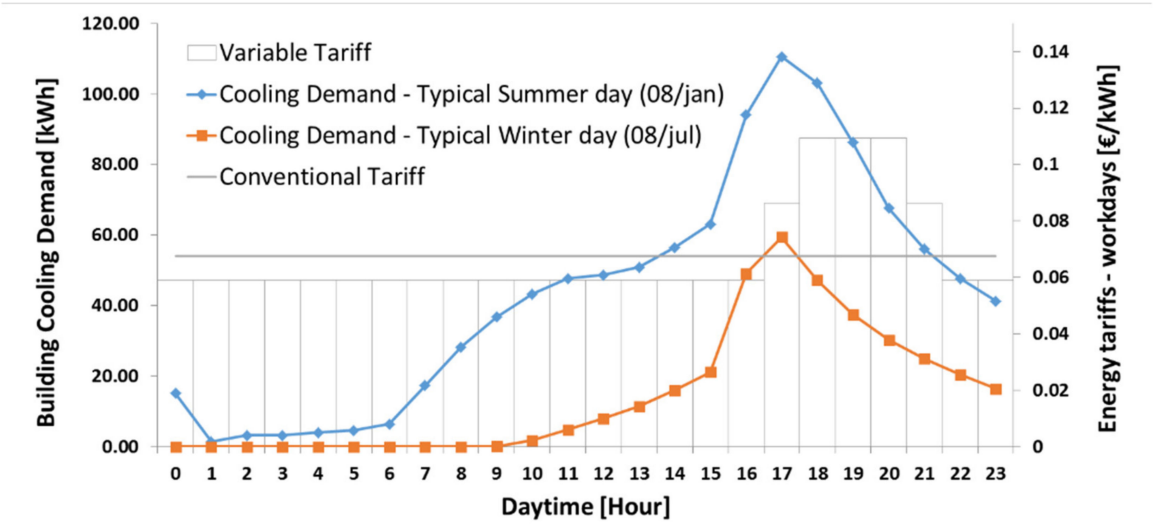

Figure A2. Building daily cooling energy demand (kWh) and energy tariffs (EUR/kWh).

Weather data files were obtained from the US National Renewable Energy Laboratory (NREL) website. The TRNSYS simulation graphics can be built for different time frames, up to 8760 h (1 year), as shown in Figure A3, allowing them to verify the cycling seasons effect on the building temperature, the cooling/heating demand compared to the exter-

nal weather conditions, or for 24 h, it can be used for the energy consumption shifting calculations.

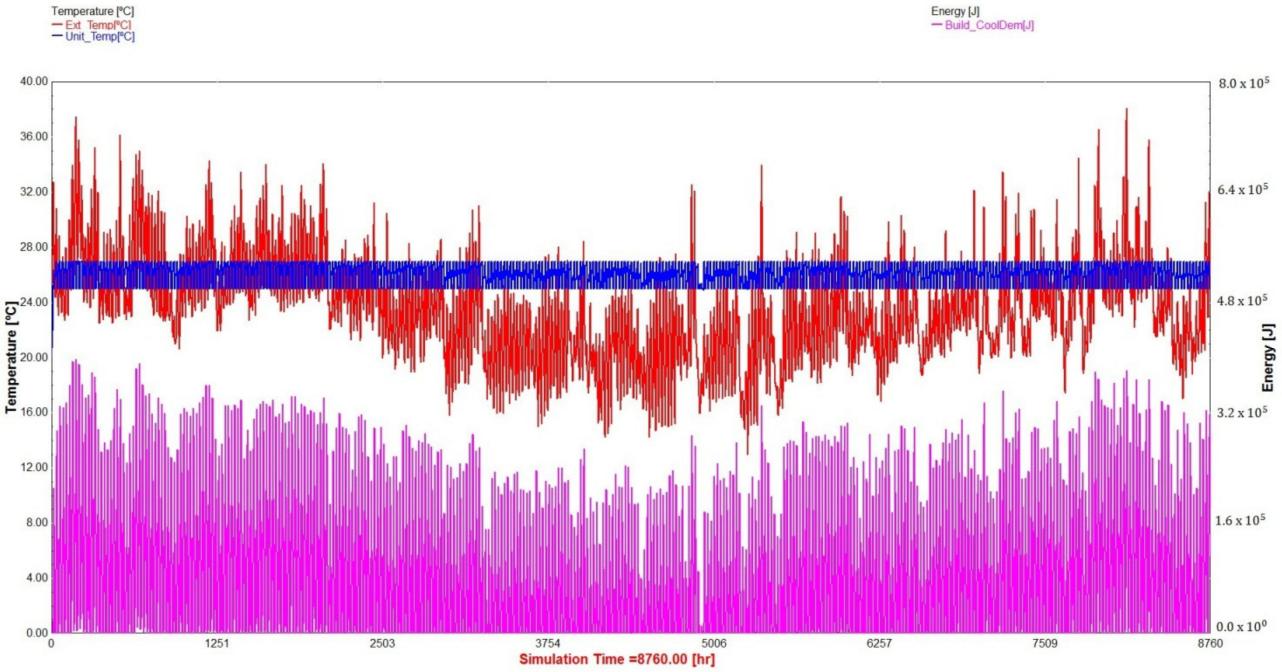

Figure A3. Annual simulation with ambient temperatures (red), comfortable inside temperatures (blue), and cooling demand (purple) for Rio de Janeiro.

Appendix D. Chillers Data

The selected chiller models for the simulations were the York YACL0043 for the Base Case and YACL0022 for the other scenarios. The partial load rates are detailed in Table A5.

Table A5. Chiller partial load data [26].

% Load	Cooling Capacity (ton)	Compressor Input Power (kW)	Ambient Temperature (°C)	Energy Efficiency Rate EER
Chiller YACL0043 31.2 Ton (110 kW)—Base Case and Scenario 1				
100	31.2	31.7	35.0	10.7
75	25.1	19.5	28.5	13.2
50	17.6	10.7	20.4	17.1
25	9.7	4.6	12.8	21.5
Chiller YACL0022 15.6 Ton (56 kW)—Scenarios 2 and 3				
100	15.6	17.6	35.0	10.3
50	9.7	5.6	20.4	18.8
1 ton = 12,000 Btu/h = 3.517 kW = 12,660.67 kJ/h				

Appendix E. Chiller Calculation Comparison

Using industry standard sizing, rule of thumb [25], in Equation (A1), it is possible to verify how the modeling and simulation allow for obtaining the most accuracy on the sizing of equipment.

$$400 \left[\frac{ft^2}{ton}\right] = 37 \left[\frac{m^2}{ton}\right] \quad (A1)$$

The building cooled area, 2520 m^2 or 27,125 ft^2, results in a chiller of about 68.1 ton, oversized compared to that calculated through the TRNSYS model.

Appendix F. Summary of Symbols and Indexes Used in the Equations and Diagrams

BUI_IN: Building Cooled Water Input (m^3/h)
BUI_OUT: Building Cooled Water Output (m^3/h)
CH_{Cap_n}: Chiller Capacity (n = 0, 1, 2, 3; n = 0 for Base Case; n = 1, 2, 3 for Scenarios 1, 2, 3) (kW) or (ton)
CH_{Sch} : Chiller Schedule Signal ($0 \leq$ signal ≤ 1)
CH_IN: Chiller Input (Water to be Cooled) (m^3/h)
CH_OUT: Chiller Output (Cooled Water) (m^3/h)
CO: Conventional Tariff—Power: (EUR/kW); Energy: (EUR/kWh)
C_p : Specific Heat for water [kWh/kg°C]
C_t: Sum of all relevant costs occurring in year t (EUR)
D_{TES} : TES diameter [m]
ΔT: Cool Coil temperature difference ($T_{out} - T_{in}$) (°C)
DV_n: Flow Diverter (n = 1, 2)
DV_n_IN_p: Flow Diverter Input (n = 1, 2; p = 1, 2) (m^3/h)
DV_n_OUT_p: Flow Diverter Output (n = 1, 2; p = 1, 2) (m^3/h)
F_{rMax} = Pump Fçow Rate Capacity (kg/h) or (m^3/h);
H_{TES} : TES height [m]
i = Nominal Discount Rate (%)
I = General Energy Price Inflation (%).
LOOP_1: Chiller Side Water Loop
LOOP_2: Building Side Water Loop
m: Water mass (kg)
N: Length of study period (years);
Optm. Ct. Pw.: Optimal Value for the Contracted Power from the grid (kW)
P_n_IN: Water Pump Input (n = 1, 2) (m^3/h)
P_n_OUT: Water Pump Output (n = 1, 2) (m^3/h)
Q_{BCD} : Building Cooling Demand [kWh]
$Q_{Build\_max\_d}$: Building maximum cooling demand (kWh/day);
ρ: Water density (kg/m^3)
r = Real Discount Rate (%)
T_{in} : Input Cool Coil Water Temperature (°C)
T_n: Tee Piece (n = 1, 2)
T_{out} : Output Cool Coil Water Temperature (°C)
TES_IN_n: TES Water Input (n = 1, 2) (m^3/h)
TES_OUT_n: TES Water Output (n = 1, 2) (m^3/h)
Total Pw.: Building Total Power Demanded (kW)
VT: Variable Tariff—Power: [€/kW]; Energy: (EUR/kWh)
V_{TES}: TES volume (m^3)
Ych: Chiller Control Signal ($0 \leq$ signal ≤ 1)
Yp_n: Water Pump Control Signal (n = 1, 2; $0 \leq$ signal ≤ 1)
α_n: Flow Diverter Control Signal (n = 1, 2; $0 \leq$ signal ≤ 1)

Appendix G. TRNSYS Simulations and Optimizations Results. Base Case and Scenarios

Table A6. Simulation results—Base Case and Scenarios 1 to 3.

	No PV							PV (No Energy Exportation)							PV (Energy Esportation—Net Metering)					
						CO [1]	VT [2]		CO			VT				CO			VT	
	Chiller Cap ton	Chiller Cap kW	Chiller Inv EUR × 10^3	TES Vol m^3	TES Inv EUR × 10^3	LCC 20y EUR × 10^3	LCC 20y EUR × 10^3	PV (×7) NoExp	PV Inv EUR × 10^3	LCC 20y EUR × 10^3	PV (×7) NoExp	PV Inv EUR × 10^3	LCC 20y EUR × 10^3	PV (×7) EnExp	PV Inv EUR × 10^3	LCC 20y EUR × 10^3	PV (×7) EnExp	PV Inv EUR × 10^3	LCC 20y EUR × 10^3
BCase	30.17	106.10	16.9	0	0	151.8 [3]	150.3	13	13.6	142.1	12	12.6	143.6	39	40.8	120.0	39	40.8	127.6
Scen 1	32.52	114.37	18.2	137.46	13.6	173.7	159.1	10	10.5	167.6	9	9.4	155.1	41	42.9	142.5	40	41.9	138.1
Scen 2	15.08	53.06	8.4	110.07	11.0	134.4	133.0	12	12.6	126.1	12	12.6	127.4	38	39.8	105.3	38	39.8	112.9
Scen 3	15.67	55.11	8.8	110.07	11.0	137.8	133.7	12	12.6	129.3	12	12.6	128.0	37	39.8	105.9	37	39.8	113.9

Investment => chiller = 560 EUR/ton; TES = 100 EUR/m^3; PV = 0.68 EUR/Wp // maintenance => chiller = 8.72 EUR/ton; TES = 0.08 EUR/m^3; PV = 0.02 EUR/Wp (annual); [1]—CO = conventional tariff; [2]—VT = variable tariff; [3]—LCC of Base Case.

References

1. Chen, Y.; Xu, P.; Gu, J.; Schmidt, F.; Li, W. Measures to improve energy demand flexibility in buildings for demand response (DR): A review. *Energy Build.* **2018**, *177*, 125–139. [CrossRef]
2. Asano, H.; Takahashi, M.; Ymaguchi, N. Market potential and development of automated demand response system. In Proceedings of the IEEE Power and Energy Society General Meeting, Detroit, MI, USA, 24–28 July 2011; pp. 1–4. [CrossRef]
3. Fiorentini, M.; Cooper, P.; Ma, Z. Development and optimization of an innovative HVAC system with integrated PVT and PCM thermal storage for a net-zero energy retrofitted house. *Energy Build.* **2015**, *94*, 21–32. [CrossRef]
4. Hirsch, A.; Okada, D.; Pless, S.; Antia, P. The role of modeling when designing for absolute energy use intensity requirements in a design-build framework. *ASHRAE Trans.* **2011**, *117 Pt 1*, 398–405.
5. Sehar, F.; Pipattanasomporn, M.; Rahman, S. An energy management model to study energy and peak power savings from PV and storage in demand responsive buildings. *Appl. Energy* **2016**, *173*, 406–417. [CrossRef]
6. Sivaneasan, B.; Kandasamy, N.K.; Lim, M.L.; Goh, K.P. A new demand response algorithm for solar PV intermittency management. *Appl. Energy* **2018**, *218*, 36–45. [CrossRef]
7. Solano, J.C.; Olivieri, L. Assessing the potential of PV hybrid systems to cover HVAC loads in a grid- connected residential building through intelligent control. *Appl. Energy* **2017**, *206*, 249–266. [CrossRef]
8. Pombeiro, H.; Machado, M.J.; Silva, C. Dynamic programming and genetic algorithms to control an HVAC system: Maximizing thermal comfort and minimizing cost with PV production and storage. *Sustain. Cities Soc.* **2017**, *34*, 228–238. [CrossRef]
9. Yu, Z. (Jerry); Chen, J.; Sun, Y.; Zhang, G. A GA-based system sizing method for net-zero energy buildings considering multi-criteria performance requirements under parameter uncertainties. *Energy Build.* **2016**, *129*, 524–534. [CrossRef]
10. Dwyer, A.; Lemire, N.; Lindhal, P.A.; Marks, P.C.; Patton, M.P. *ASHRAE Handbook HVAC Systams and Equipment*; American Society of Heating, Refrigerating and Air-Conditioning Engineers, Inc.: Norcross, GA, USA, 2016; p. 955.
11. TRNSYS. Transient System Simulation Tool. 2021. Available online: http://www.trnsys.com/index.html (accessed on 1 March 2021).
12. Durillon, B.; Davigny, A.; Kazmierczak, S.; Barry, H.; Saudemont, C.; Robyns, B. Demand Response Methodology Applied on Three-Axis Constructed Consumers Profiles. In Proceedings of the 2019 International Conference on Smart Energy Systems and Technologies (SEST), Porto, Portugal, 9–11 September 2019. [CrossRef]
13. Li, S.; Joe, J.; Hu, J.; Karava, P. System identification and model-predictive control of office buildings with integrated photovoltaic-thermal collectors, radiant floor heating and active thermal storage. *Sol. Energy* **2015**, *113*, 139–157. [CrossRef]
14. Sehar, F.; Rahman, S.; Pipattanasomporn, M. Impacts of ice storage on electrical energy consumptions in office buildings. *Energy Build.* **2012**, *51*, 255–262. [CrossRef]
15. Parameshwaran, R.; Kalaiselvam, S.; Harikrishnan, S.; Elayaperumal, A. Sustainable thermal energy storage technologies for buildings: A review. *Renew. Sustain. Energy Rev.* **2012**, *16*, 2394–2433. [CrossRef]
16. Heier, J.; Bales, C.; Martin, V. Combining thermal energy storage with buildings—A review. *Renew. Sustain. Energy Rev.* **2015**, *42*, 1305–1325. [CrossRef]
17. Hasnain, S.M. Review on sustainable thermal energy storage technologies, part II: Cool thermal storage. *Energy Convers. Manag.* **1998**, *39*, 1139–1153. [CrossRef]
18. Hajji, T.E.; Kabalan, B.; Cheng, Y.; Vinot, E.; Dumand, C. Sensitivity Analysis on the Sizing Parameters of a Series-Parallel HEV. *IFAC-PapersOnLine* **2019**, *52*, 405–410. [CrossRef]
19. Zheng, Y.; He, H.; Xu, X.; Jiang, Y. Sensitivity analysis of the hybrid electrical vehicle power system parameters. In Proceedings of the 2011 IEEE International Conference on Computer Science and Automation Engineering, Shanghai, China, 10–12 June 2011; Volume 2, pp. 601–604. [CrossRef]
20. Stroe, N.; Olaru, S.; Colin, G.; Ben-Cherif, K.; Chamaillard, Y. A two-layer predictive control for hybrid electric vehicles energy management. *IFAC-PapersOnLine* **2017**, *50*, 10058–10064. [CrossRef]
21. Sözer, H.; Takmaz, D. Calculation of the sensitivity factors within the defined indexes in a building level. *J. Sustain. Dev. Energy Water Environ. Syst.* **2020**, *8*, 1–21. [CrossRef]
22. Ministerio de Fomento (España). Documento Básico HE Ahorro de Energía 2019. Available online: http://www.arquitectura-tecnica.com/hit/Hit2016-2/DBHE.pdf (accessed on 31 March 2020).
23. Ministerio de Industria Energía y Turismo. Real Decreto 216/2014. *Bol. Estado* **2014**, *77*, 27397–27428. Available online: https://www.boe.es/boe/dias/2014/03/29/pdfs/BOE-A-2014-3376.pdf (accessed on 1 March 2021).
24. Brazilian National Electrical Energy Agency. White Tariff; ANNEL:Brazil 2017. Available online: http://www.aneel.gov.br/tarifa-branca (accessed on 1 March 2021).
25. Burdick, A. *Strategy Guideline: Accurate Heating and Cooling Load Calculations*; National Renewable Energy Laboratory (NREL): Golden, CO, USA, 2011.
26. York. Model Ycal Air-Cooled Scroll Chillers with Brazed Plate Heat Exchangers. Available online: https://www.york.com/commercial-equipment/chilled-water-systems/air-cooled-chillers/ycal_ch/ycal-scroll-chiller (accessed on 1 March 2021).
27. Solico Tanks. Solico Panel Tank Catalogue. 2016. Available online: http://solicotanks.com/wp-content/uploads/2016/01/Solico-Panel-Tank-Catalogue-2016.pdf (accessed on 1 March 2021).

28. Rismanchi, B.; Saidur, R.; Masjuki, H.H.; Mahlia, T.M.I. Energetic, economic and environmental benefits of utilizing the ice thermal storage systems for office building applications. *Energy Build.* **2012**, *50*, 347–354. [CrossRef]
29. Sharp. Sharp3000 3 kW Solar System Panel Specifications. Available online: https://www.originenergy.com.au/content/dam/origin/residential/docs/solar/legacy-models/Sharp3000_Panel_Specifications.pdf (accessed on 1 March 2021).
30. NATA Accredited Laboratories. Solar Inverters List. Available online: http://www.opti-solar.com/download/certification/inverters%20list%20100818.pdf (accessed on 4 May 2021).
31. De Soto, W.; Klein, S.A.; Beckman, W.A. Improvement and validation of a model for photovoltaic array performance. *Sol. Energy* **2006**, *80*, 78–88. [CrossRef]
32. Feldman, D.; Fu, R.; Margolis, R.; Woodhouse, M.; Ardani, K.; Fu, R.; Feldman, D.; Margolis, R.; Woodhouse, M.; Ardani, K.U.S. *Solar Photovoltaic System and Energy Storage Cost Benchmark: Q1 2020*; National Renewable Energy Lab (NREL): Golden, CO, USA, 2021; pp. 1–120. Available online: www.nrel.gov/publications.%0Ahttps://www.nrel.gov/docs/fy21osti/77324.pdf (accessed on 15 March 2021).
33. PoloAr. Fujitsu Air Conditioning Catalog. 2021. Available online: https://www.poloar.com.br/ar-condicionado/inverter/12000-btus?map=c,c,c (accessed on 1 March 2021).
34. López Prol, J.; Steininger, K.W. Photovoltaic self-consumption regulation in Spain: Profitability analysis and alternative regulation schemes. *Energy Policy* **2017**, *108*, 742–754. [CrossRef]
35. Schneider, F. *What's in a Methodology?* Leiden University: Leiden, The Netherlands, 2014; Available online: http://www.politicseastasia.com/studying/whats-methodology/ (accessed on 1 March 2020).
36. Rudestam, K.E.; Newton, R.R. The method chapter: Describing your research plan. In *Surviving Your Dissertation: A Comprehensive Guide to Content and Process*; Michigan University: Ann Arbor, MI, USA, 2007; pp. 87–116. Available online: http://books.google.com/books?id=vmWdAAAAMAAJ&pgis=1 (accessed on 10 March 2020).
37. Schachinger, D.; Gaida, S.; Kastner, W.; Petrushevski, F.; Reinthaler, C.; Sipetic, M.; Zucker, G. An Advanced Data Analytics Framework for Energy Efficiency in Buildings. In Proceedings of the 2016 IEEE 21st International Conference on Emerging Technologies and Factory Automation (ETFA), Berlin, Germany, 6–9 September 2016; pp. 31–34.
38. Friedrich, L.; Afshari, A. Framework for Energy Efficiency White Certificates in the Emirate of Abu Dhabi. *Energy Procedia* **2015**, *75*, 2589–2595. [CrossRef]
39. Satchwell, A.J.; Cappers, P.A.; Deason, J.; Forrester, S.P.; Frick, N.M.; Gerke, B.F.; Ann Piette, M. A conceptual framework to describe energy efficiency and demand response interactions. *Energies* **2020**, *13*, 4336. [CrossRef]
40. Iskin, I.; Daim, T.U. Technology assessment for energy efficiency programs in Pacific Northwest. In Proceedings of the 2014 Portland International Center for Management of Engineering and Technology; Infrastructure and Service Integration, Kanazawa, Japan, 27–31 July 2014; pp. 498–506. Available online: https://www.scopus.com/inward/record.uri?eid=2-s2.0-84910150009&partnerID=40&md5=bb159bd6925fb827b63e27f66b8ba7d4 (accessed on 10 March 2020).
41. Energy Plus. Weather Data. Available online: https://energyplus.net/weather-location/europe_wmo_region_6/ (accessed on 1 March 2019).